A Novel Interaction of the Golgi Complex with the Vimentin Intermediate Filament Cytoskeleton

Ya-sheng Gao and Elizabeth Sztul

Department of Cell Biology, University of Alabama at Birmingham, Birmingham, Alabama 35294

Abstract. The integration of the vimentin intermediate filament (IF) cytoskeleton and cellular organelles in vivo is an incompletely understood process, and the identities of proteins participating in such events are largely unknown. Here, we show that the Golgi complex interacts with the vimentin IF cytoskeleton, and that the Golgi protein formiminotransferase cyclodeaminase (FTCD) participates in this interaction. We show that the peripherally associated Golgi protein FTCD binds directly to vimentin subunits and to polymerized vimentin filaments in vivo and in vitro. Expression of FTCD in cultured cells results in the formation of extensive FTCD-containing fibers originating from the Golgi region, and is paralleled by a dramatic rearrangements of the vimentin IF cytoskeleton in a coordinate process in which vimentin filaments and FTCD integrate into chimeric fibers. Formation of the FTCD fibers is obligatorily coupled to vimentin assembly and does not occur in vim$^{-/-}$ cells. The FTCD-mediated regulation of vimentin IF is not a secondary effect of changes in the microtubule or the actin cytoskeletons, since those cytoskeletal systems appear unaffected by FTCD expression. The assembly of the FTCD/vimentin fibers causes a coordinate change in the structure of the Golgi complex and results in Golgi fragmentation into individual elements that are tethered to the FTCD/vimentin fibers. The observed interaction of Golgi elements with vimentin filaments and the ability of FTCD to specifically interacts with both Golgi membrane and vimentin filaments and promote their association suggest that FTCD might be a candidate protein integrating the Golgi compartment with the IF cytoskeleton.

Key words: FTCD • vimentin • intermediate filaments • Golgi complex • IFAP

Introduction

Intermediate filaments (IFs)[1] constitute one of the three major cytoskeletal systems of eukaryotic cells. IFs are composed of a diverse but related family of proteins whose expression patterns are usually cell type specific (Fuchs and Weber, 1994). Distinct groups of IFs are described based on their assembly properties, gene structure, and sequence homologies: the keratins, the neurofilament-like proteins, the lamins, and the vimentin-related proteins. The vimentin-related group includes vimentin, desmin, glial fibrillary acid protein (GFAP), and peripherin. Vimentin is expressed predominantly in cells of mesenchymal origin (Franke et al., 1982) and in cells adopted to culture (Franke et al., 1979). Desmin is required for normal myofibrillogenesis and resistance to contractile damage in muscle cells, since knockout mice lacking desmin exhibit cardiovascular lesions and skeletal myopathy (Li et al., 1994; Milner et al., 1996). The functional significance of the GFAP and vimentin IF cytoskeletons are less clear. Knockout of GFAP (Gomi et al., 1995; Pekny et al., 1995) or vimentin (Colucci-Guyon et al., 1994) produces animals that are live and overall normal, suggesting that elimination of these IF elements can either be compensated by other cytoskeletal arrays or that they perform more subtle cellular functions. However, GFAP-lacking mice show changes in myelination of axons and GFAP assembly (Galou et al., 1996; Liedtke et al., 1996; Shibuki et al., 1996), whereas vimentin null animals show changes in recovery from neuronal injury (Pekny et al., 1999) and, at the cellular level, changes in fat granule deposition (Lieber and Evans, 1996), glycolipid processing (Gillard et al., 1998), and movement of low density lipoprotein–derived cholesterol (Sarria et al., 1992).

Numerous IF-associated proteins (IFAPs) have been described that appear to connect IFs to the actin cytoskeleton, to the microtubule cytoskeleton, to cell–cell and

Address correspondence to Elizabeth Sztul, Department of Cell Biology, University of Alabama at Birmingham, McCallum Building, Rm. 668, 1530 S. Third Ave., Birmingham, AL 35294-0005. Tel.: (205) 934-1465. Fax: (205) 975-9131. E-mail: esztul@uab.edu

[1]*Abbreviations used in this paper:* FTCD, formiminotransferase cyclodeaminase; GFAP, glial fibrillary acid protein; GFP, green fluorescent protein; IF, intermediate filament; IFAP, IF-associated protein; MTOC, microtubule-organizing center; NC, nitrocellulose; NRK, normal rat kidney; SG, stacked Golgi.

cell–substratum adhesion zones, and to cellular membranes (Stappenbeck and Green, 1992; Stappenbeck et al., 1993; Yang et al., 1996; for review see Chou et al., 1997; Correia et al., 1999; Leung et al., 1999; Yang et al., 1999). The list of IFAPs that specifically associate with vimentin has been growing and now includes plectin (involved in cross-linking vimentin IFs to other cytoskeletal elements and to specialized membrane adhesion sites), filamin (an actin binding protein that is likely to cross-link IFs to actin cytoskeleton), fimbrin (an actin-binding protein possibly involved in attaching IFs to cell–substrate adhesion sites), kinesin (involved in linking IFs to microtubules), transglutaminase (possibly involved in cross-linking vimentin subunits or filaments), and various chaperones and kinases (functions of which are not well understood at present). In addition, vimentin IFs have been shown in electron microscopic studies to lie in close spatial association with specific membranous organelles such as the nucleus, the plasma membrane, mitochondria, and the Golgi complex (Katsumoto et al., 1991; for review see Georgatos and Maison, 1996). However, whether IFs are merely adjacent to these organelles or are directly tethered by binding to as yet unidentified surface IFAPs has not been resolved.

Here, we present the initial report of a direct association between the Golgi complex and the vimentin IF cytoskeleton. The association is apparent in vivo, with Golgi elements aligned on vimentin filaments clustered around the microtubule-organizing center (MTOC). The microtubule cytoskeleton is not required for the IF–Golgi association, and dispersed Golgi ministacks remain associated with vimentin filaments in cells in which microtubules are disrupted. Direct binding between recombinant vimentin and isolated Golgi elements can be also demonstrated by centrifugation and solid phase binding assays in vitro.

We document that the enzyme formiminotransferase cyclodeaminase (FTCD) localizes to the Golgi complex and the vimentin IF cytoskeleton in vivo, and that FTCD directly interacts with vimentin filaments and Golgi membranes in vitro. FTCD has been shown by us (Gao et al., 1998) and others (Bashour and Bloom, 1998; Hennig et al., 1998) to be identical to the 58K Golgi protein, initially proposed to link Golgi membranes to the microtubule cytoskeleton (Bloom and Brashear, 1989). However, recent reexamination of FTCD behavior indicates that FTCD binds to polyglutamated residues preferentially found in brain tubulin and does not interact with tubulin from other sources (Bashour and Bloom, 1998). FTCD is found in every cell type examined, but its expression is orders of magnitude higher in the liver than in other tissues or cell types (Bashour and Bloom, 1998; Hennig et al., 1998; Solans et al., 2000). It is likely that within hepatocytes, FTCD has predominantly a metabolic function, catalyzing two sequential reactions in the histidine degradation pathway. The FT domain of this bifunctional enzyme first transfers the formimino group of formiminoglutamate to tetrahydrofolate to produce formiminotetrahydrofolate and glutamate, and then the CD domain catalyzes the cyclization of the folate intermediate to produce methenyltetrahydrofolate and releasing ammonia (for review see Shane and Stokstad, 1984). However, the function of FTCD in tissues and cells that are not major sites for histidine metabolism has not been explored. We now report that FTCD facilitates interactions between the Golgi complex and the IF cytoskeleton. We show that FTCD promotes the binding of isolated Golgi elements to vimentin in vitro, and that expression of FTCD in vivo dramatically changes the overall structure of the vimentin IF cytoskeleton and causes a coordinate disruption of Golgi structure. Based on our results, we propose that FTCD is a candidate linker protein connecting the Golgi complex to the vimentin IF cytoskeleton.

Materials and Methods

Reagents and Antibodies

Restriction enzymes and molecular reagents were from Promega, New England BioLabs, Inc., or QIAGEN. Rat liver λ ZAP II cDNA expression library and Pfu DNA polymerase were from Stratagene. All other chemicals were from Sigma-Aldrich or Fisher Scientific. A hybridoma cell line (58K-9) was a gift of Dr. George Bloom (University of Texas Southwestern Medical Center, Dallas, TX) and was used to generate ascites in mice. IgGs were purified from ascites by affinity adsorption as described previously (Gao et al., 1998). Polyclonal rabbit serum raised against porcine FTCD was a gift of Dr. Robert MacKenzie (McGill University, Montreal, Quebec). mAbs against vimentin (clone V9) and against β-tubulin (clone TUB 2.1) were from Sigma-Aldrich. mAb to mouse vimentin (clone 9.5) was provided by Dr. Robert Evans (University of Colorado, Denver, CO). Polyclonal goat antibody against human vimentin was from ICN Biomedicals. Polyclonal rabbit antibodies against GM130 have been described previously (Nelson et al., 1998). Monoclonal antigiantin antibody was a kind gift of Dr. Hans-Peter Hauri (University of Basel, Basel, Switzerland). Oregon green–labeled goat anti–rabbit IgG antibody, Texas red–labeled goat anti–mouse IgG antibody, FITC-labeled goat anti–mouse IgM antibody, Texas red–labeled goat anti–rabbit IgG antibody were from Molecular Probes, Inc. HRP-labeled sheep anti–rabbit IgG antibody, HRP-labeled donkey anti–mouse IgG antibody, and HRP-labeled rabbit anti–goat IgG antibody were from Amersham Pharmacia Biotech. SuperSignal West Pico chemiluminescence substrate was from Pierce Chemical Co. EIA/RIA 96-well microtiter plates were from Corning, Inc.

Cells

COS-7 cells were grown in DME with glucose and glutamine (Mediatech, Inc.) supplemented with 10% FBS (Life Technologies), 100 U/ml penicillin, and 100 μg/ml streptomycin (Life Technologies). Normal rat kidney (NRK) cells were grown in the same medium, except the concentration of FBS was 5%. Mouse cell line MFT-6 (vim^+) and the cell line MFT-16 ($vim^{-/-}$) derived from a vimentin knockout mouse were provided by Dr. Robert Evans. MFT-6 (vim^+) and MFT-16 ($vim^{-/-}$) cells were grown in 1:1 Ham's F12 (with glutamine; Mediatech, Inc.): DME (with glucose and glutamine), supplemented with 5% FBS and 10 μg/ml Gentamycin (Mediatech, Inc.). Mouse NIH3T3 cells stably expressing green fluorescent protein (GFP)–vimentin were provided by Drs. Gregg Gundersen and Ron Liem (Columbia University, New York, NY), grown in DME with 10% FBS, streptomycin, and penicillin as above, and supplemented with 300 μg/ml G418 sulfate (Life Technologies).

Subcellular Fractionation of COS-7 Cells

COS-7 cells were grown in two 150-mm dishes to 70% confluency and were transfected with 35 μg of GFP-rFTCD plasmid per plate using the calcium phosphate transfection system (Life Technologies). 48 h after transfection, cells were washed (four times, 2 min each) with prechilled HKM (25 mM Hepes, pH 7.4, 115 mM potassium acetate, 2.5 mM magnesium chloride) and scraped from plates. Collected cells (in ~1 ml solution) were supplemented with 10 μl protease inhibitor cocktail (Sigma-Aldrich) and passed through a 26G3/8 needle (Becton Dickinson) 20 times on ice. The cell lysate was centrifuged at 1,500 *g* for 10 min at 4°C. The resulting postnuclear supernatant was mixed with 2 M sucrose in HKM to a final concentration of 1.6 M sucrose. The mixture was loaded at the bottom of a centrifuge tube and overlaid with 1.3, 1.0, 0.8, and 0.5 M sucrose in HKM. Equilibrium centrifugation was carried out in SW41 Ti rotor (Beckman Coulter) at 135,000 *g* for 14 h at 4°C. Fractions were collected from the top.

DNA Cloning

Cloning and partial sequencing of rat FTCD were performed as described previously (Gao et al., 1998). A full-length FTCD clone in vector pBluescript SK(−) (Stratagene) was obtained and named rFTCD–pBS. For cloning into pcDNA 3.1(+) (Invitrogen), the full-length rFTCD cDNA was cut out from rFTCD–pBS using BamHI–XhoI sites and was inserted at the corresponding sites in pcDNA 3.1(+). The construct was named rFTCD–pcDNA. To make a chimera of GFP and FTCD (GFP–rFTCD), the coding sequence of FTCD was amplified by PCR with rFTCD–pBS as the template. A BglII site was created upstream from the start codon, and a HindIII site was created at the stop codon, destroying it. The PCR fragment was inserted into pEGFP-C2 vector (CLONTECH Laboratories, Inc.) at the BglII–HindIII sites. FTCD was at the COOH terminus of GFP and was in frame. There were seven amino acids between GFP and the first methionine of FTCD, and 18 amino acids between the last amino acid of FTCD (glutamic acid) and the new stop codon provided by the vector. A full-length FTCD was also cloned into a bacterial expression system as follows: the FTCD sequence was amplified by PCR, using rFTCD–pBS as the template, using a T7 primer as the 3′ end reverse primer and a 5′ end forward primer containing a NdeI site before the start codon. The coding portion was cut with NdeI and EcoRI from the PCR product and was cloned into pET-21b (Novagen). This construct was named rFTCD–pET.

In Vitro Transcription/Translation of FTCD

In vitro translation of rFTCD–pBS was carried out using the TNT T7-coupled reticulocyte lysate system from Promega, according to the manufacturer directions. 2 μg of rFTCD–pBS cDNA was used in a total reaction volume of 100 μl. Trans ^{35}S label from ICN Biomedicals was used as the source of [^{35}S]methionine and [^{35}S]cysteine. The reaction was carried out at 30°C for 4 h.

Expression and Purification of Recombinant FTCD from Bacteria

rFTCD–pET was transfected into BL21 (DE3) cells (Novagen) by standard protocol. A single colony was grown in 1 liter of medium at 30°C until OD_{600} reached 1.0. IPTG (Fisher Scientific) was then added to 0.5 mM, and the culture was grown for another 3 h at 30°C. The cells were collected by centrifugation at 4,500 *g* for 10 min and washed once with PBS. FTCD was purified according to a previously published protocol (Murley et al., 1993), with minor modification. All steps were performed on ice or at 4°C. In short, cells were resuspended in 0.1 M potassium phosphate (pH 7.3), 35 mM β-mercaptoethanol, and 1 mM PMSF, sonicated for 30 s for five times with 1-min intervals. The sonicated material was supplemented with Triton X-100 to 0.02% concentration, mixed and centrifuged at 27,000 *g* for 30 min. The collected supernatant was supplemented with 10% volume of 250 mM MOPS (pH 7.3) and 24% volume of glycerol, then with ammonium sulfate to 40% saturation, and precipitation was carried out with stirring overnight. The mixture was centrifuged at 27,000 *g* for 30 min, and the resulting pellet was resuspended in 5 ml buffer A (25 mM MOPS, pH 7.3, 5 mM potassium phosphate, pH 7.3, 5% glycerol, 35 mM β-mercaptoethanol, 0.02% Triton X-100, and 1 mM PMSF, which was added freshly). The resuspended pellet was dialyzed two times against 500 ml buffer A and clarified at 27,000 *g* for 30 min. The resulting supernatant was loaded onto a 1.6- × 18-cm DEAE Sepharose Fast Flow (Amersham Pharmacia Biotech) column equilibrated with buffer A. Proteins were eluted with a linear gradient of buffer A and equal volume of 0.3 M potassium chloride in buffer A at 22 ml/h. Collected fractions were analyzed by SDS-PAGE and immunoblotting with anti-FTCD antibodies. The formiminotransferase activity of DEAE-purified FTCD was comparable to that of purified pig FTCD (data not shown; Murley et al., 1993). The DEAE-purified FTCD was further purified using Cibacron blue 3Ga column followed by a Heparin column, according to a previously described protocol (Murley et al., 1993). Collected fractions were analyzed by SDS-PAGE and immunoblotting with anti-FTCD antibodies. Fractions containing the peak of FTCD by immunoblotting were pooled and analyzed by SDS-PAGE and Coomassie brilliant blue R-250 staining (see Fig. 2 A).

Transfections and Immunofluorescence Microscopy

COS-7 cells were transfected with the calcium phosphate transfection system (Life Technologies) or with TransIT polyamine transfection reagents (Mirus Corporation), according to manufacturer protocols. Other cells were transfected with the TransIT polyamine transfection reagent. 18–48 h after transfection, cells were fixed with 3% paraformaldehyde and processed for immunofluorescence microscopy as previously described (Alvarez et al., 1999). In some experiments, the cells were fixed and permeabilized with −20°C methanol for 20 min at −20°C. All following steps were as described (Alvarez et al., 1999). Actin filaments were visualized by labeling with phalloidin-FITC (Molecular Probes, Inc.) diluted with 0.4% fish skin gelatin, 0.05% Tween 20 in PBS. In some cases, cells were treated with nocodazole (Sigma-Aldrich) at 10 μg/ml from a 10 mg/ml DMSO stock. The treatment was at 37°C for periods indicated in figure legends. In experiments analyzing the localization of endogenous FTCD and vimentin, COS-7 cells were first washed with prechilled HKM buffer and then treated with 40 μg/ml digitonin in HKM for 5 min on ice (Plutner et al., 1992), followed by washing with HKM (three times, 2 min each) and fixing with 3% paraformaldehyde as above.

SDS-PAGE and Immunoblotting

Samples were analyzed by SDS-PAGE as described previously (Sztul et al., 1985). After SDS-PAGE, proteins were transferred to NitroPure nitrocellulose (NC) membrane (Micron Separations Inc.), and the membrane was subjected to immunoblotting as previously described (Gao et al., 1998). In some cases, NC membranes were striped at 50°C for 30 min in 62.5 mM Tris-HCl (pH 6.7), 100 mM β-mercaptoethanol, and 2% SDS, washed with 0.05% Tween 20 in TBS (TBS-T), blocked in 7.5% nonfat milk–TBS-T, and reprobed with another antibody.

Overlay Assay

Proteins were analyzed by SDS-PAGE and were transferred to NC membrane, which was blocked with 1% BSA–HKM-0.05% Tween 20. The membrane was then incubated for 2 h at room temperature with 40 μl in vitro transcribed/translated FTCD diluted in the blocking buffer. After washing with HKM, the membrane was dried in air and exposed to X-ray film.

Expression and Purification of Recombinant Mouse Vimentin from Bacteria

Plasmid pCMV-Vim, a gift from Dr. Robert Evans was used as the PCR template. A NdeI and a BamHI site were introduced at the 5′ and the 3′ end of the coding region of vimentin. The amplified cDNA was then cloned into pET-21b vector and transfected into BL21 (DE3) cells as described above. Induction was with 0.5 mM IPTG at 37°C for 3.5 h. Vimentin purification was carried out according to the method described previously (Domingo et al., 1991). In short, bacteria were collected and treated with lysozyme and DNase I. Cells were lysed with a detergent buffer (20 mM Tris-HCl, pH 7.5, 0.2 M NaCl, 1% deoxycholic acid, 1% NP-40, 10 mM NaF, and 2 mM EDTA). Inclusion bodies were recovered by centrifugation at 5,000 *g* for 15 min at 4°C. After washing with Triton buffer (10 mM Tris-HCl, pH 7.5, 0.5% Triton X-100, 1 mM EDTA, 0.1 M NaCl), the inclusion bodies were dissolved in urea solution (8 M urea in 50 mM Tris-HCl and 10 mM DTT, pH 8.0). The solubilized material was loaded on a DEAE–Sepharose Fast Flow column (2.6 × 18 cm), which had been equilibrated with urea solution, and was eluted with a linear NaCl gradient from 0–500 mM made in urea solution. Fractions enriched in vimentin were pooled, and proteins were precipitated with solid ammonium sulfate to 60% saturation. The precipitates were collected by centrifugation at 25,000 *g* for 15 min, redissolved in urea solution, and dialyzed against 10 mM Tris-HCl (pH 7.4) and 0.1% β-mercaptoethanol. The dialyzed vimentin was further centrifuged at 100,000 *g* in type 60Ti rotor (Beckman Coulter) for 30 min at 4°C to clear precipitates. Vimentin was recovered in the supernatant and was ≥95% pure as judged by Coomassie blue staining of an SDS-PAGE gel.

Binding of FTCD to Vimentin Filaments

To avoid nonspecific sedimentation, all protein materials used in binding experiments were preclarified at 125,000 *g* for 30 min at 20°C. To polymerize vimentin filaments, recombinant mouse vimentin at ~2 mg/ml was mixed with NaCl to a final concentration of 0.15 M NaCl and incubated in a 35°C waterbath for 40 min. For in vitro association, 4 μg preformed vimentin filaments was incubated with buffer or with different amounts of bacterially expressed and purified FTCD. In some experiments 0.25 μg BSA in buffer was used as a control. The reactions were carried out at room temperature for 2.5 h in 20 μl solution that also contained 25 mM Hepes (pH 7.4), 115 mM potassium acetate, 5 mM β-mercaptoethanol,

0.02% Triton X-100, and 2% glycerol. The mixtures were then centrifuged at 100,000 *g* in TLA 45 rotor (Beckman Coulter) at 20°C for 30 min. Supernatants and pellets were recovered, and equal amounts of supernatants and pellets were processed for SDS-PAGE and immunoblotting with anti-FTCD antibodies. The amount of material loaded on the gel was adjusted so that a similar amount of FTCD was analyzed in each binding group. An analogous binding experiment was carried out for EM, except that 0.06 μg recombinant FTCD was used. After incubation, the solution was applied to Farmvar-coated grids and stained with 1% uranyl acetate. The samples were examined on a Hitachi 7000 transmission electron microscope at accelerating voltage of 75 kV.

Binding of Vimentin to Golgi Elements

Rat liver stacked Golgi (SG) fraction was isolated as described before (Nelson et al., 1998). The SG fraction was made 40% nycodenz (Life Technologies) in HKM and overlaid with 36 and 32% nycodenz–HKM. Upfloatation was carried out in SW50.1 rotor (Beckman Coulter) at 135,000 *g* for 7 h. Enriched Golgi fractions were identified by immunoblotting with anti-GM130 antibodies. The fractions were pooled, and the protein concentration was ~650 μg/ml. 100-μl Golgi fraction was diluted with 170 μl HKM buffer and then supplemented either with 5 μl buffer or 5 μl buffer containing 10 μg purified recombinant mouse vimentin. The mixtures were incubated at 4°C for 3 h, supplemented with 2 M sucrose in HKM to a final sucrose concentration of 1.6 M, and were loaded at a bottom of centrifuge tubes. The load was overlaid with 1.3 and 0.8 M sucrose in HKM, and the tubes were centrifuged in SW 50.1 rotor at ~135,000 *g* for 7 h. Fractions were collected from top of the gradient. Fractions 3 and 4 were pooled, supplemented with 2 M sucrose in HKM to 1.6 M final concentration, and subjected to another round of equilibrium centrifugation as described above.

In experiments to test the ability of FTCD to promote Golgi–vimentin association, Golgi elements isolated by upfloatation in a nycodenz gradient (see above) were first incubated with bacterially expressed and purified FTCD for 3 h at 4°C. BL21 (DE3) bacterial lysate without FTCD was used in control incubations. The mixtures were adjusted to 1.6 M sucrose (final concentration) in HKM and loaded on the bottom of centrifuge tubes. The samples were overlaid with 1.3 and 0.8 M sucrose in HKM and subjected to equilibrium centrifugation at 135,000 *g* for 16 h in SW 50.1 rotor at 4°C. Fractions were collected from the top, processed for SDS-PAGE, and immunoblotted with anti-GM130 antibodies. GM130-containing fractions were combined and incubated with vimentin for 3 h at 4°C. The mixtures were adjusted to 1.6 M sucrose final concentration and loaded at bottoms of tubes, overlaid with 0.8 and 1.3 M sucrose in HKM, and subjected to another round of equilibrium centrifugation as described above. Fractions were collected and analyzed as described above.

Solid Phase Binding Assays: Binding of FTCD to Vimentin

A 96-well RIA/EIA plate was coated with 1 mg/ml poly-L-lysine (Sigma-Aldrich) in water (75 μl/well) for 20 min at room temperature. The plate was washed with water, and 50 μl of buffer (10 mM Tris-HCl, pH 7.4) or bacterially expressed and purified mouse vimentin at 20 μg/ml in the same buffer was added to each well. Each experiment group was done in triplicate. The plate was incubated at 32°C for 2 h and washed once with HK (25 mM Hepes, 115 mM potassium acetate, pH 7.4). The plate was blocked with 1% BSA–HK (100 μl/well) for 1 h at 32°C and then washed with HK two times. Bacterially expressed and purified FTCD was first diluted to 3 μg/ml in 1% BSA–HK, and then supplemented with goat anti-vimentin serum or with nonimmune goat serum (serum dilution was 1:15), and the mixtures were added to wells. The plate was incubated for 2 h at 32°C and washed with HK (five times, 2 min each). The bound material was recovered from each well with 50 μl SDS-PAGE sample buffer. Solutions from the triplicate wells were pooled. Equal volume of samples from each group was analyzed by immunoblotting using rabbit anti–pig FTCD antibody.

FTCD-mediated Binding of Golgi Elements to Vimentin

The plate was coated with poly-L-lysine, incubated with vimentin, and blocked with BSA–HK as described above. Each experimental group had four wells. Bacterially expressed and purified FTCD was diluted with 1% BSA–HK to 3 or 1 μg/ml and added to the plate. Control group received only 1% BSA–HK. The plate was incubated for 2 h at 32°C and washed with HK four times. Isolated Golgi elements were diluted in 1% BSA–HK to 80 μg/ml, and 50 μl was loaded per well. Control wells received only 1% BSA–HK. The plate was incubated at room temperature for 2 h and washed with HK. All wells received 50 μl monoclonal antigiantin antibodies diluted in 1% BSA–HK, and the plate was incubated for 1 h at room temperature, washed, and further incubated with 50 μl of HRP-labeled secondary anti–mouse antibody for 1 h at room temperature. After washing with HK four times, all wells received 50 μl of 1 mg/ml OPD substrate (Pierce Chemical Co.). The color was developed for 20 min and then stopped by adding 50 μl of H_2SO_4 to each well.

Results

FTCD Colocalizes with Golgi Elements and with Vimentin IFs

Prior immunofluorescence studies have shown that FTCD (previously called the 58K protein) localizes to the Golgi region in cultured cells from various species and tissue origin (Donaldson et al., 1990; Lippincott-Schwartz et al., 1990; Vaisberg et al., 1996). In agreement, endogenous FTCD colocalizes with the Golgi protein marker GM130 in COS-7 cells (Fig. 1 A). However, the level of colocalization was not perfect, and FTCD signal extended beyond the region labeled with anti-GM130 antibodies. This finding agrees with the incomplete colocalization between FTCD and Golgi markers in DU249 chicken hepatoma cells (Hennig et al., 1998) and suggests that, in addition to binding to the Golgi, FTCD also associates with other cellular structures that lie close to, but do not perfectly overlap with, the Golgi stack. Since the cytoplasmic non-Golgi FTCD staining appeared slightly filamentous, we examined FTCD distribution in NIH3T3 cells stably expressing GFP-tagged vimentin. As shown in Fig. 1 B, FTCD was detected in a typical Golgi pattern (arrows) and in filamentous extensions where it colocalized with vimentin filaments (arrowheads). Similarly, careful analysis of FTCD and endogenous vimentin distribution in the periphery of COS-7 cells showed that FTCD is localized along vimentin filaments (Fig. 1 C, arrowheads). FTCD localization to the Golgi and to vimentin IFs was also seen in other cultured cells (data not shown), indicating the commonality of this distribution.

The unexpected colocalization of FTCD with vimentin filaments suggested that FTCD might interact directly or indirectly with the vimentin IF cytoskeleton.

FTCD Binds Directly to Vimentin IFs

To test whether FTCD and vimentin associate, bacterially expressed and purified FTCD (Fig. 2 A) was tested for its ability to bind to polymerized recombinant vimentin filaments in a centrifugation-based assay. Under the centrifugation conditions used, vimentin filaments were recovered exclusively in the pellet (data not shown). In contrast, bacterially expressed FTCD is soluble and is recovered exclusively in the supernatant following centrifugation in the absence of vimentin filaments (Fig. 2 B, lanes 5 and 6). However, when vimentin filaments are added to FTCD (in different FTCD/vimentin ratios), significant proportions of FTCD bind to the filaments and are recovered in the pellets (lanes 1–4). In this experiment, FTCD is detected by immunoblotting since monomeric FTCD and vimentin comigrate on SDS-PAGE. To ensure that the signal is FTCD, a control incubation lacking FTCD was analyzed

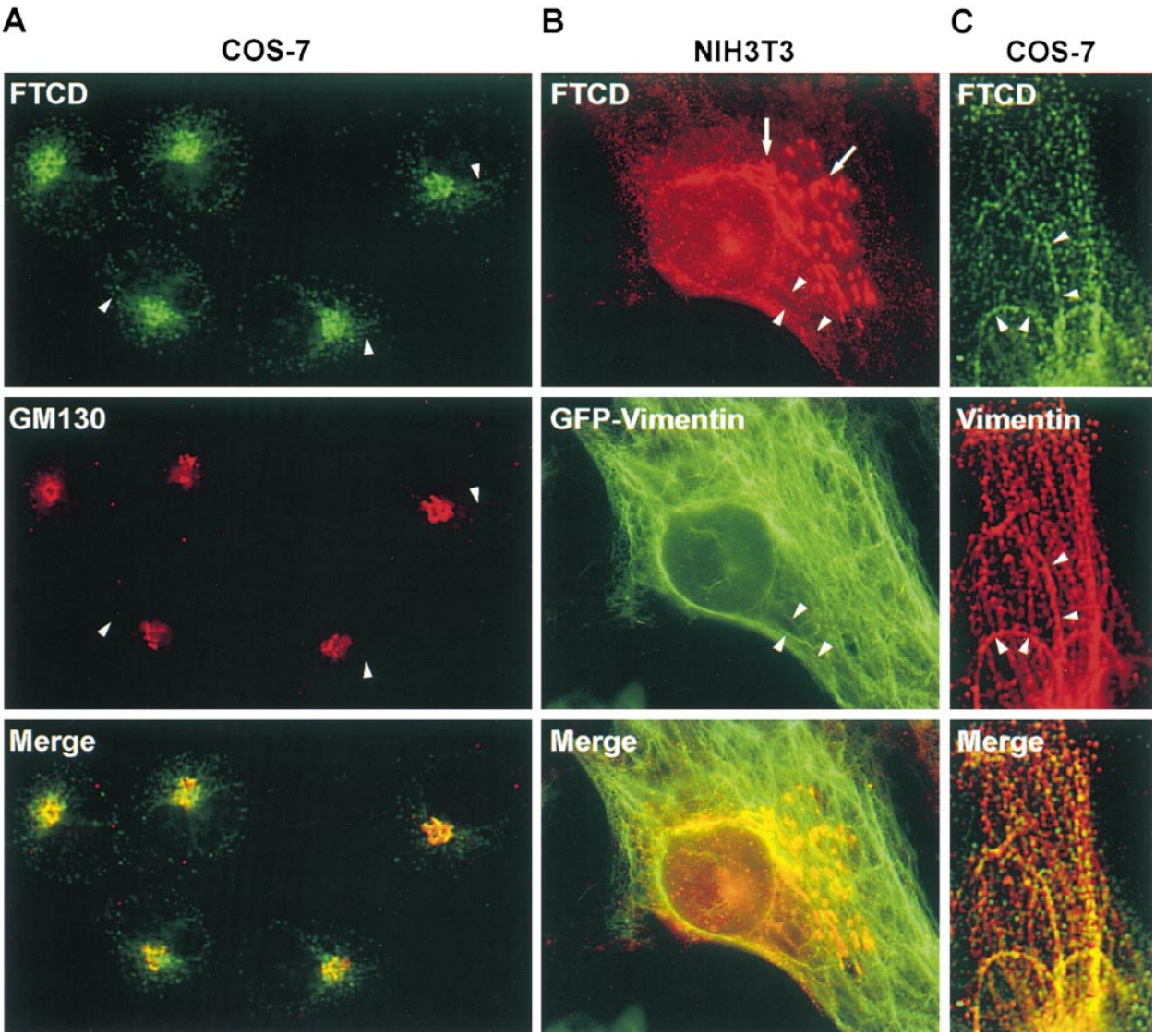

Figure 1. Endogenous FTCD localizes to Golgi elements and to vimentin IFs. (A) COS-7 cells were processed for immunofluorescence using monoclonal anti-FTCD (FTCD) and polyclonal anti-GM130 (GM130) antibodies. FTCD colocalizes with the Golgi marker GM130 but is also present in areas lacking GM130 (arrowheads). (B) NIH3T3 cells stably expressing GFP–vimentin were processed for immunofluorescence using monoclonal anti-FTCD antibodies. FTCD localizes to Golgi elements (arrows) and to vimentin filaments (arrowheads). (C) COS-7 cells were processed for immunofluorescence using polyclonal anti-FTCD and monoclonal anti-vimentin antibodies. FTCD localizes to vimentin filaments in cell periphery (arrowheads).

and shows no signal (Fig. 2 B, lanes 7 and 8). To confirm that FTCD binding to vimentin filaments is specific, and does not represent trapping within the filament meshwork, pelleting of BSA was tested as a control. As shown in a Coomassie brilliant blue–stained gel in Fig. 2 C, BSA did not pellet with the vimentin filaments.

To morphologically examine FTCD binding to vimentin, polymerized vimentin filaments were incubated with bacterially expressed and purified FTCD (FTCD used in this and all of the following experiments is analogous to that in Fig. 2 A) and analyzed by EM. As control, polymerized filaments without FTCD were analyzed. As shown in Fig. 2 D, and previously described (Nikolic et al., 1996), vimentin filaments appear as a loose meshwork of ~10-nm smooth filaments after staining with uranyl acetate. In contrast, vimentin filaments incubated with FTCD appear bumpy, and are decorated with spherical structures irregularly spaced along the filaments (Fig. 2 E). The spherical structures in the boxed region are shown at higher magnification in Fig. 2 F and have dimensions (~12 nm) consistent with the previously reported size of FTCD octamers (Beaudet and Mackenzie, 1976). Significantly, the addition of FTCD resulted in more compacted and dense filamentous aggregates. Often, spherical FTCD structures were observed in between two parallel filaments (Fig. 2 G, arrows) or at intersections of filaments (data not shown), suggesting that FTCD might bundle vimentin filaments.

To confirm the FTCD-vimentin interaction, and to test whether FTCD can bind to subunit vimentin, FTCD overlay assay was carried out. Bacterially expressed and purified FTCD, BSA, and recombinant vimentin were sub-

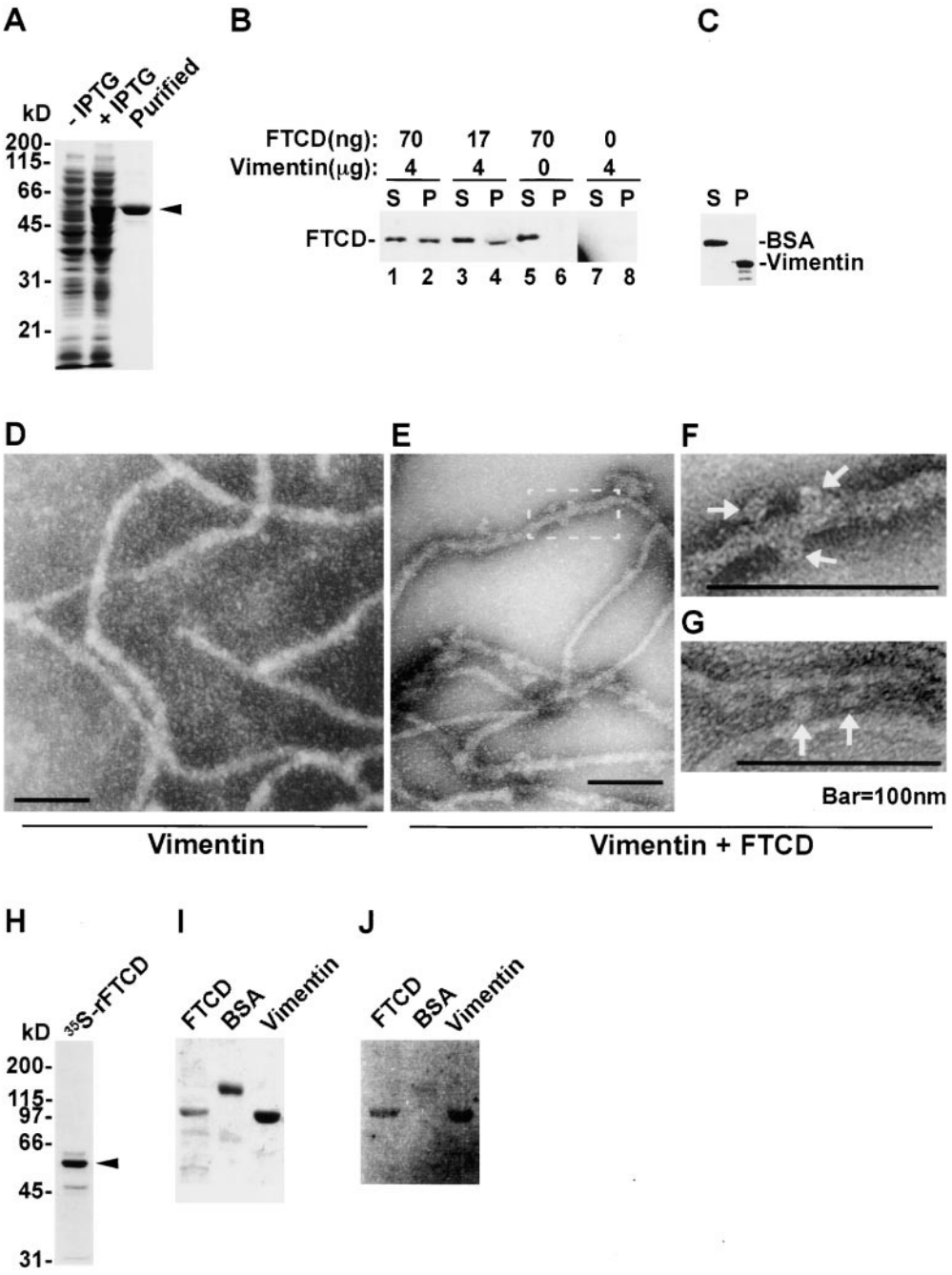

Figure 2. FTCD binds directly to vimentin IFs. (A) FTCD expression was induced by IPTG in bacteria, and FTCD was purified as described in Materials and Methods. A Coomassie blue–stained gel shows a major 58-kD FTCD band (arrowhead). (B) Bacterially expressed and purified FTCD was mixed in different ratios with polymerized vimentin filaments and centrifuged at 100,000 *g* for 30 min at 20°C. The supernatants and pellets were recovered, and an equivalent proportion of each was processed by SDS-PAGE. The proteins were transferred to NC and immunoblotted with polyclonal anti-FTCD antibodies. FTCD remains soluble in the absence of vimentin filaments (lanes 5 and 6), but pellets when vimentin filaments are added (lanes 1 to 4). In lanes 7 and 8, only vimentin without added FTCD was processed. (C) BSA was incubated with vimentin filaments, and the mixture was centrifuged as above. The supernatant and pellet were recovered, and an equivalent proportion of each was processed by SDS-PAGE and Coomassie blue staining. BSA does not bind to and is not recovered with vimentin filaments. (D–G) Vimentin filaments alone (Vimentin) or incubated with bacterially expressed and purified FTCD (Vimentin + FTCD) were stained with uranyl acetate and visualized by EM. In the vimentin only sample, the filaments appear smooth (D), whereas filaments incubated with FTCD are decorated with spherical structures (E). A higher magnification of the area in E, is shown in F. The size of the spherical structures is ~12 nm (arrows) and is consistent with the size of FTCD octomers. The spherical structures were often seen linking individual vimentin filaments (G, arrows). (H) rFTCD–pBS was used as template in an in vitro transcription/translation reaction. A fluorograph of generated products shows a major 58-kD protein (arrowhead). (I) Bacterially expressed and purified FTCD, BSA and bacterially expressed and purified mouse vimentin were processed by SDS-PAGE, and the gel stained with Coomassie blue to show relative amounts of proteins. (J) A gel analogous to that in I was transferred to NC and overlaid with ^{35}S-FTCD, as generated in H. Radiolabeled FTCD binds directly and specifically to FTCD and vimentin. Bar, 100 nm.

jected to SDS-PAGE and are shown in a Coomassie blue–stained gel in Fig. 2 I. An analogous gel was transferred to NC membrane and overlaid with ^{35}S-radiolabeled FTCD generated in vitro by coupled transcription/translation (Fig. 2 H). As shown in the fluorograph in Fig. 2 J, radiolabeled FTCD preferentially bound to FTCD and vimentin. Binding to FTCD was expected since FTCD homooligomerizes to form the native octomeric structure (Findlay and MacKenzie, 1987). Quantitation of the relative amounts of each protein in I and the relative amounts of ^{35}S-FTCD bound to each protein in J showed that ~6-fold more radiolabeled FTCD bound to FTCD than to BSA, and ~10-fold more radiolabeled FTCD bound to vimentin than to BSA.

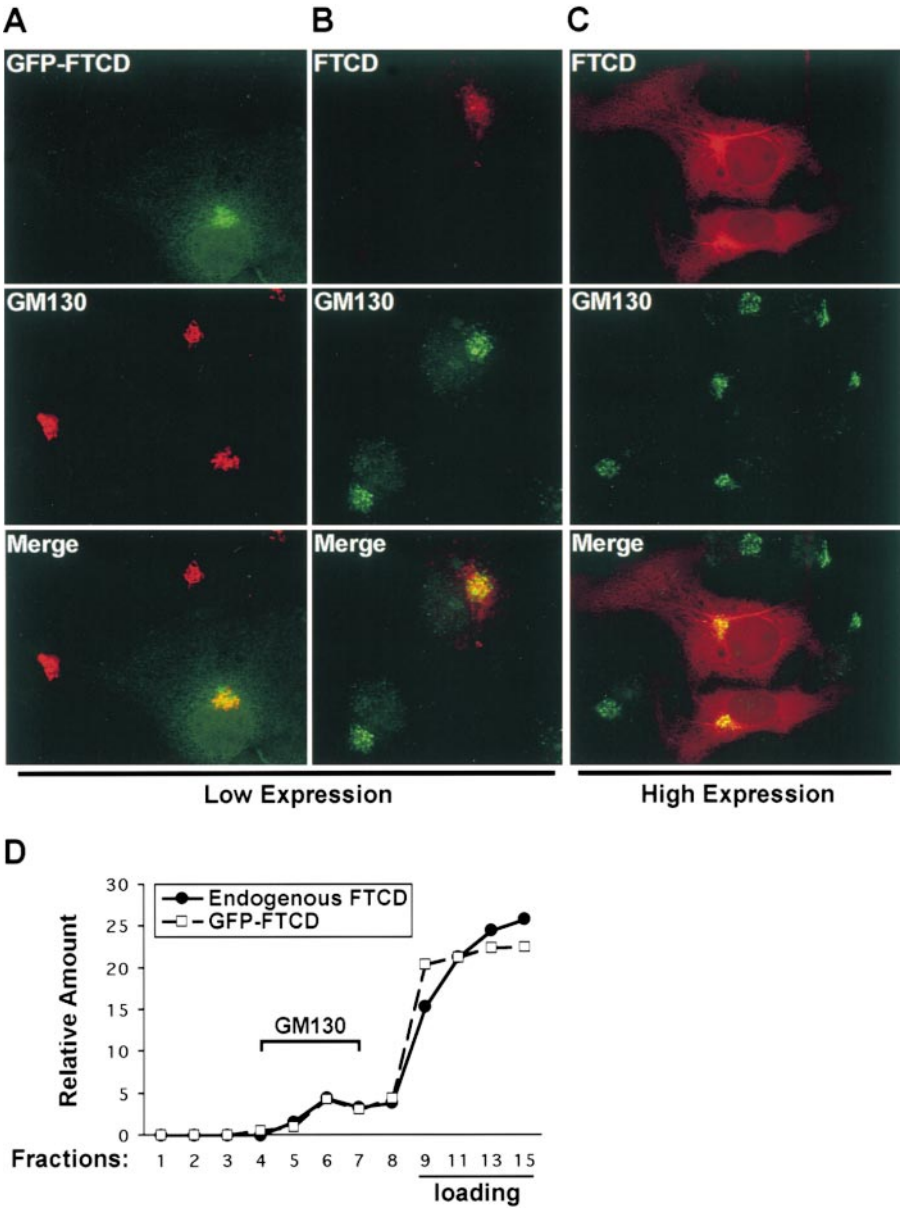

Figure 3. FTCD targets to the Golgi complex and organelles into fibers. COS-7 cells were transfected with GFP-tagged (A) or -untagged (B and C) rFTCD and grown for 18–48 h. (A) Cells were processed for immunofluorescence with polyclonal anti-GM130 antibodies. (B and C) Cells were processed for immunofluorescence with monoclonal anti-FTCD and polyclonal anti-GM130 antibodies. In cells expressing low levels of FTCD (A and B), the recombinant FTCD is concentrated in the Golgi region. In cells expressing high levels of FTCD (C), the recombinant FTCD also localizes to thick fibers originating from the Golgi region. (D) COS-7 cells were transfected with GFP–FTCD for 48 h and fractionated by equilibrium density centrifugation. An equivalent amount of each fraction was processed by SDS-PAGE, transferred to NC, and immunoblotted with anti-FTCD antibodies to detect the 58-kD endogenous FTCD and the 86-kD recombinant GFP–FTCD. The NC was also probed with anti-GM130 antibodies. The relative recovery of endogenous FTCD, GFP–FTCD, and GM130 in each lane were quantitatively evaluated by densitometry. Endogenous FTCD and GFP–FTCD were predominantly recovered in the high density sucrose load (fractions 9–15) containing soluble cytosolic proteins. A proportion of FTCD and GFP–FTCD were recovered in low density sucrose (fractions 5–7) enriched in the Golgi marker GM130.

The biochemical and morphological data document the novel association of FTCD with vimentin subunits and with assembled vimentin filaments. Together, our results show that FTCD interacts with the Golgi complex and with the vimentin IF cytoskeleton, suggesting that FTCD might participate in these cellular components.

FTCD Mediates Remodelling of the Vimentin IF Cytoskeleton

To initiate the inquiry into the intracellular function of FTCD, we transiently expressed GFP-tagged and -untagged full-length FTCD in COS-7 cells. As shown in Fig. 3 A, in cells expressing low levels of GFP–FTCD, the recombinant protein was predominantly localized to the Golgi area, where it colocalized with GM130. In addition, faint filamentous staining extending from the Golgi region in a pattern similar to that of endogenous FTCD was detected. The faithfulness of GFP–FTCD distribution was also analyzed by fractionation after cell disruption. As shown in Fig. 3 D, the distribution of GFP–FTCD paralleled that of endogenous FTCD. Both were predominantly recovered at the bottom of the gradient (fractions 9–15), representing the high density sucrose load and containing soluble cytosolic proteins. Only a small amount of GFP–FTCD and endogenous FTCD was recovered in the low density sucrose (fractions 5–7) enriched in the Golgi membrane marker GM130. These results are analogous to those seen following homogenization of rat liver, where FTCD was predominantly found in the cytosolic fraction, with only a small proportion (<10%) cofractionating with Golgi membranes (Bloom and Brashear, 1989; Gao et al., 1998).

To ensure that the observed distribution of GFP–FTCD was not influenced by the GFP part of the chimera, untagged FTCD was expressed in COS-7 cells, and its localization was detected with anti-FTCD antibodies. In this and all other experiments involving recombinant FTCD transfections, anti-FTCD antibodies were used at a high dilution adjusted to detect only the recombinant but not the

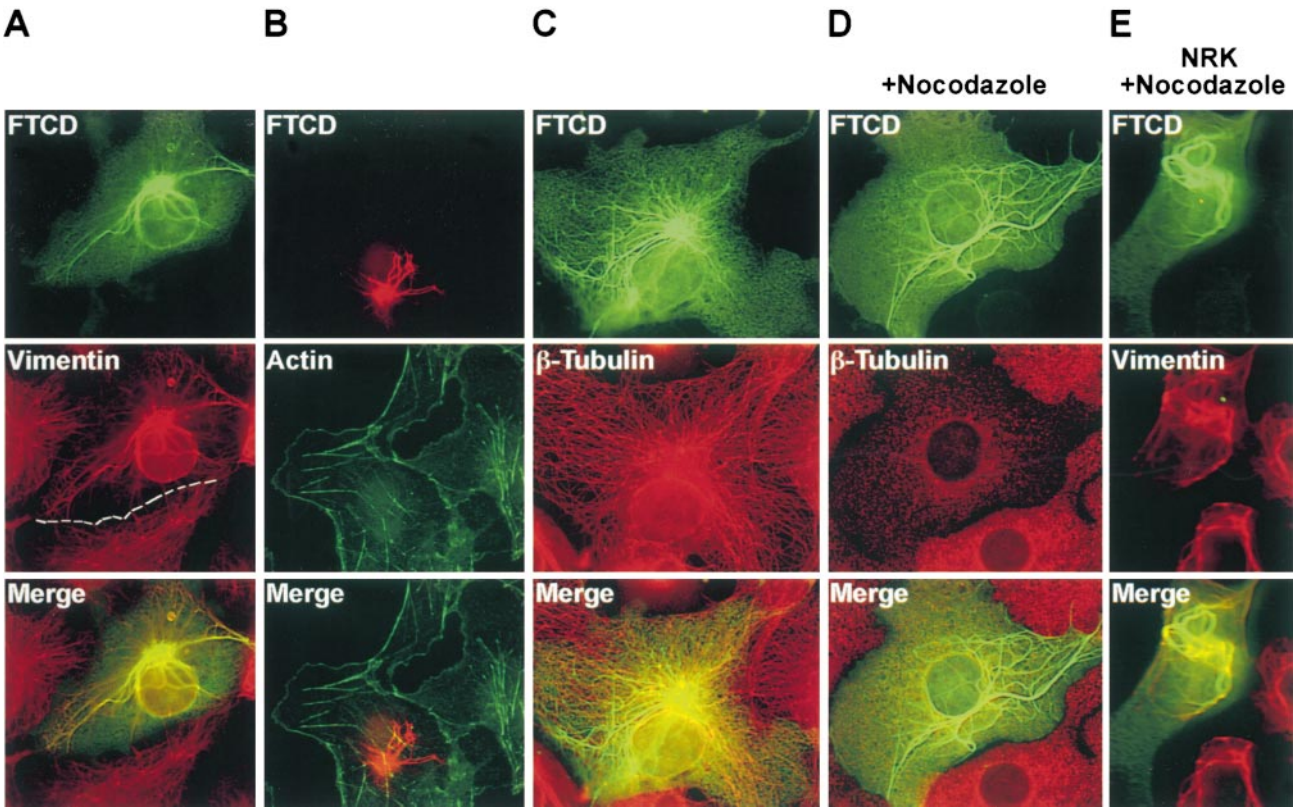

Figure 4. FTCD remodels the vimentin IF cytoskeleton independent of the actin and the microtubule cytoskeletons. COS-7 cells (A–D) or NRK cells (E) were transfected with rFTCD–pcDNA, grown for 48 h, and processed for immunofluorescence. (A) Cells were labeled with polyclonal anti-FTCD and monoclonal antivimentin antibodies. The border of a transfected cell is outlined by dashed lines. The vimentin cytoskeleton is perturbed in the transfected cell colocalizes with vimentin to thick fibers originating from the Golgi region. (B) Cells were labeled with polyclonal anti-FTCD antibodies and phalloidin–FITC. Actin distribution in the transfected cell is indistinguishable from that in untransfected cells. (C) Cells were labeled with polyclonal anti-FTCD and monoclonal anti–β-tubulin antibodies. The microtubule pattern in transfected cells is indistinguishable from that in untransfected cells. (D) Cells were treated with 10 μg/ml nocodazole for 3 h at 37°C, then labeled with polyclonal anti-FTCD and monoclonal anti–β-tubulin antibodies. FTCD fibers persist despite the disruption of the microtubular network. (E) Cells were treated with 10 μg/ml nocodazole for 3 h at 37°C, and then labeled with polyclonal anti-FTCD and monoclonal antivimentin antibodies. FTCD/vimentin fibers persist despite the disruption of the microtubular network.

endogenous FTCD. As shown in Fig. 3 B, in cells expressing low levels of FTCD, the recombinant protein predominantly localized to GM130-containing Golgi elements and to adjacent filamentous structures. The distribution was indistinguishable from that of endogenous FTCD and GFP-tagged FTCD. A different pattern was observed in cells expressing higher levels of recombinant FTCD, where filamentous structures originating from the Golgi region were significantly more pronounced (Fig. 3 C). In addition, the fibers appeared thicker and more disorganized. Based on the finding that FTCD interacts directly with vimentin filaments, we examined if the thick filamentous structures contain vimentin.

As shown in Fig. 4 A, in COS-7 cells expressing high levels of FTCD, dramatic processes positive for FTCD and for vimentin were apparent. This pattern was observed in many cells, and quantitation of cells 48 h after transfection showed that ~70% of transfected cells contained extensive FTCD fibers. The FTCD fibers originated from the peri-Golgi region and radiated outwards towards the cell periphery. Exact colocalization of FTCD and vimentin was observed in all fibers. In all cases, vimentin IFs were disfigured to a different extent, from mild thickening of the normally delicate filaments to the formation of very thick bundles. In the latter case, most of the cellular vimentin appeared integrated into the bundles, resulting in a marked depletion of vimentin filaments from the cell periphery (dash lines mark the border of a transfected cell in Fig. 4 A). To ensure that the formation of the FTCD/vimentin fibers was not an artifact of expressing rat FTCD in a particular simian COS-7 background, we transfected the rat FTCD construct into various mammalian cells. Analogous fibrillar FTCD/vimentin structures were seen in transfected human, rat, and mouse cells (Figs. 4 E and 5 B; and data not shown).

Together, the data indicate that FTCD interacts with and drastically modulates the structure of the vimentin IF cytoskeleton.

FTCD-mediated Remodelling of the Vimentin IF Cytoskeleton Does Not Involve Changes in the Actin or the Microtubule Cytoskeletons

The IF cytoskeleton physically and functionally interacts with the two other cellular cytoskeletons composed of ac-

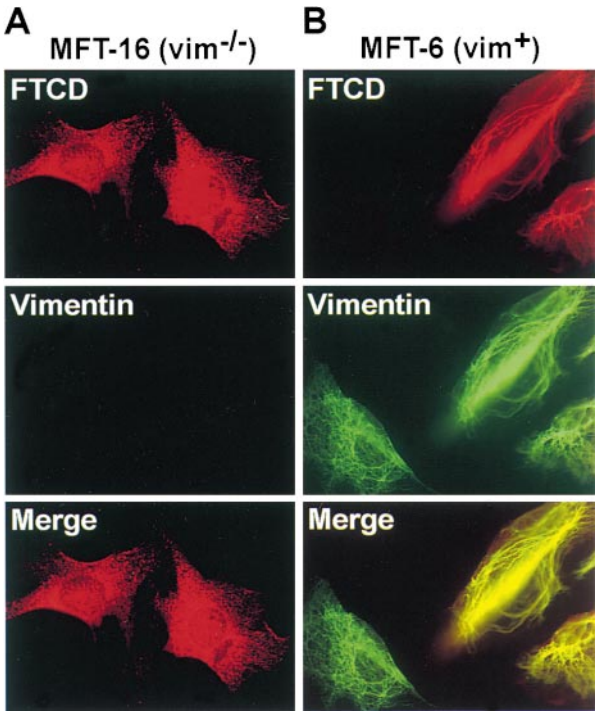

Figure 5. FTCD fiber formation requires vimentin IFs. MFT-16 cells derived from a vimentin knockout mouse and lacking vimentin ($vim^{-/-}$) and MFT-6 cells derived from a normal litter mate and containing vimentin (vim^{+}) were transfected with rFTCD–pcDNA. 48 h later, cells were processed for immunofluorescence using polyclonal anti-FTCD and monoclonal antivimentin antibodies. FTCD/vimentin fibers form only in the vim^{+} cells, whereas FTCD remains diffusely distributed in the $vim^{-/-}$ cells.

tin filaments and microtubules (Blose et al., 1984; Svitkina et al., 1996; Yang et al., 1996, 1999; Liao and Gundersen, 1998; Prahlad et al., 1998; Correia et al., 1999). The IF architecture appears to be at least partially regulated by the other cytoskeletal systems, as shown, for example, by the coordinate collapse of IFs following the disruption of the microtubule cytoskeleton by drug treatments or by injection of antitubulin and antikinesin antibodies (Blose et al., 1984; Gyoeva and Gelfand, 1991; Svitkina et al., 1996). Therefore, we examined whether the observed changes in vimentin IFs could be due to effects of FTCD overexpression on the actin and/or the microtubule cytoskeleton. As shown in Fig. 4 B, cells expressing recombinant FTCD contained normal cortical actin and actin cables and stress fibers, indistinguishable from those in the neighboring untransfected cells. Furthermore, the FTCD fibers did not colocalize with actin-containing structures, suggesting that the remodelling of the IF cytoskeleton has no marked effect on the integrity of the actin cytoskeleton. In agreement, rFTCD–pcDNA-transfected cells showed no change in cell shape or ability to adhere to the substrate.

Similarly, the microtubule cytoskeleton of a rFTCD–pcDNA-transfected cell is not visibly altered from that seen in adjacent untransfected cells (Fig. 4 C). Microtubule distribution was largely undisturbed even in cells where drastic rearrangement of IFs had occurred. FTCD fibers and microtubules often appeared in close juxtaposition, paralleling but not exactly colocalizing with each other. Because of this close apposition and the previously described microtubule-dependent kinesin-based extension of peripheral IFs (Gyoeva and Gelfand, 1991; Liao and Gundersen, 1998; Kreitzer et al., 1999), we explored whether the maintenance of the FTCD/vimentin fibers was dependent on the presence of an intact microtubule cytoskeleton. Cells were treated with the microtubule depolymerizing drug nocodazole, and the fate of microtubules and the FTCD fibers was monitored by double label immunofluorescence. As shown in Fig. 4, D and E, FTCD/vimentin fibers persisted in the nocodazole-treated cells, despite the complete disruption of the microtubule cytoskeleton. These results indicate that assembled FTCD/vimentin fibers are relatively stable, and their maintenance is independent of the microtubule cytoskeleton. Similarly, microtubules were not stabilized by the FTCD/vimentin fibers. Together, the data indicate that FTCD exerts its effects on the vimentin IF cytoskeleton directly, without disrupting the actin or the microtubule cytoskeletons.

FTCD Mediates Fiber Formation Only in the Presence of Cellular Vimentin

The colocalization of FTCD and vimentin in the fibers could represent an independent assembly of FTCD and vimentin into filaments and a subsequent linking to form chimeric fibers. To explore whether the formation of the FTCD fibers can occur independently of vimentin or is obligatorily coupled to the coassembly of vimentin into the same structure, a vimentin-minus ($vim^{-/-}$) cell line (MFT-16) derived from a vimentin knockout mouse (Colucci-Guyon et al., 1994; Svitkina et al., 1996; Holwell et al., 1997) was transfected with rFTCD–pcDNA, and the distribution of recombinant FTCD was analyzed. As a control, a vimentin-plus (vim^{+}) cell line (MFT-6) derived from a normal litter mate of the knockout mouse was similarly analyzed. As shown in Fig. 5 A, recombinant FTCD appeared uniformly distributed throughout the cytoplasm and did not form fibers in the MFT-16 ($vim^{-/-}$) cells. In contrast, extensive fibers were visible in the MFT-6 (vim^{+}) control cell line (Fig. 5 B). The overall morphology of the FTCD/vimentin fibers in the MFT-6 cells was indistinguishable from those in COS-7 or NRK cells. These results indicate that the formation of the fibrous structures of FTCD is intrinsically dependent on the presence of vimentin, suggesting that FTCD and vimentin coassemble into the chimeric fibers.

FTCD Mediates Coordinate Rearrangement of Vimentin IFs and Golgi Structure

We have shown that FTCD interacts with the Golgi and binds to vimentin IFs, suggesting that the formation of FTCD/vimentin fibers might influence Golgi structure. To examine this, COS-7 cells were transfected with FTCD or GFP–FTCD to induce formation of fibers, and then Golgi structure was analyzed. A transfected cell containing numerous FTCD/vimentin fibers radiating from the perinuclear MTOC region is shown in Fig. 6 A. The overall Golgi morphology in the transfected cell is relatively normal compared with that seen in a neighboring untransfected cell, except for a tubular extension (arrowhead) projecting from the otherwise compact Golgi

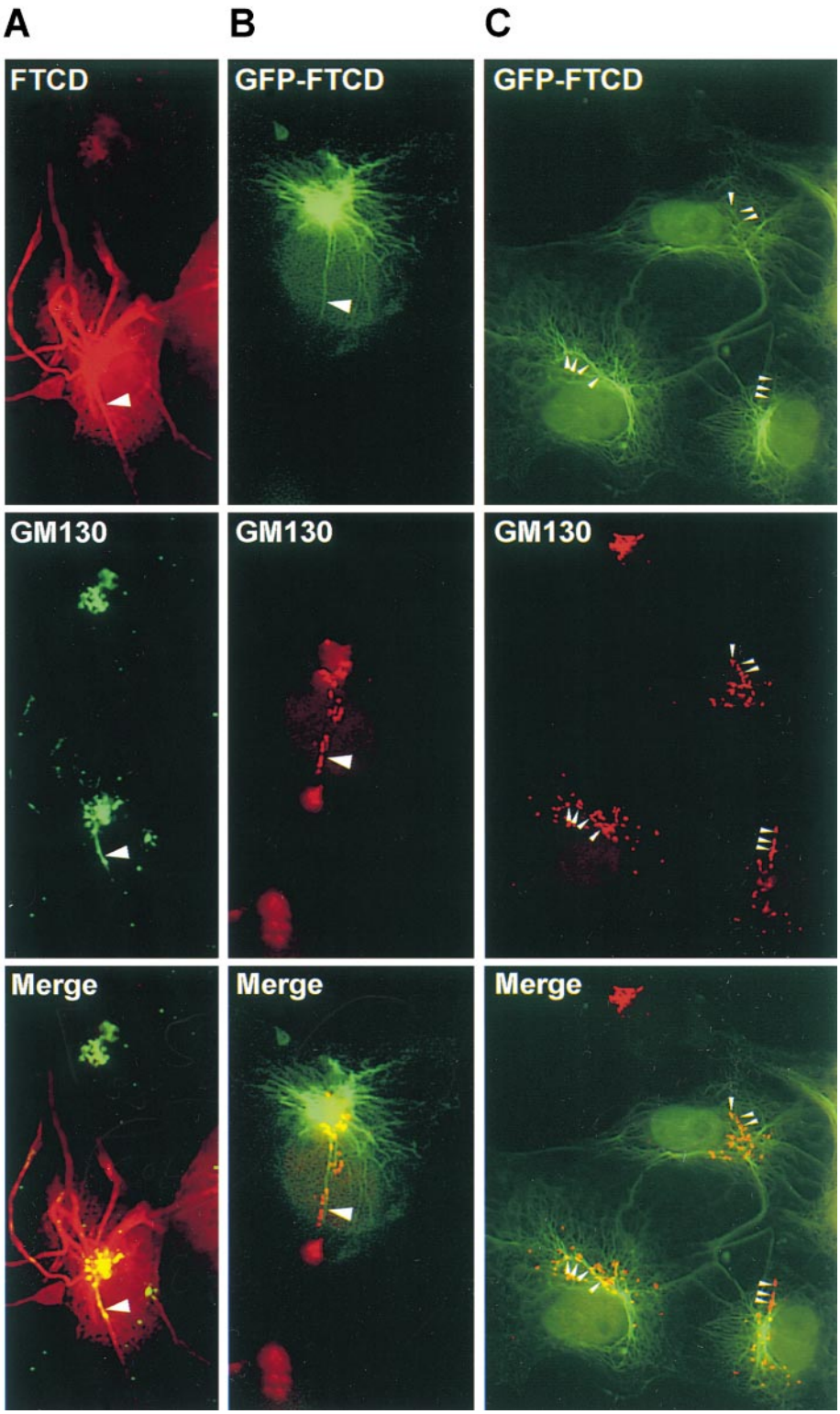

Figure 6. FTCD mediates coordinate disruption of vimentin IF cytoskeleton and Golgi structure. COS-7 cells were transfected with untagged (A) or GFP-tagged (B and C) FTCD. 48 h later, cells were processed for immunofluorescence using monoclonal anti-FTCD and polyclonal anti-GM130 antibodies (A) or only polyclonal anti-GM130 antibodies (B and C). Numerous FTCD/vimentin fibers originating from the Golgi region are evident in the transfected cells. The structure of the Golgi complex is perturbed to a varying degree in transfected cells, from a relatively normal Golgi complex containing a single tubular protrusion (arrowhead in A), to a Golgi complex with a projection fragmented into individual elements (arrowhead in B), to a completely dispersed Golgi structure (arrowheads in C). In all cases, the fragmented Golgi elements are associated with the FTCD/vimentin fibers.

complex. The Golgi extension appears aligned along one of the FTCD/vimentin fibers and precisely colocalizes with it. Such Golgi extensions were rarely observed in cells without FTCD/vimentin fibers. The unusual extensions of Golgi elements were also seen in cells containing GFP–FTCD/vimentin fibers (Fig. 6 B). In all cases, the Golgi tubules originated from the perinuclear MTOC region and were associated with the GFP–FTCD/vimentin fibers. The Golgi extensions were either continuous or, as shown in this cell, fragmented into individual elements (arrowhead). Significantly, all Golgi fragments were aligned on the FTCD/vimentin fiber. The Golgi fragmentation was often extreme, and many cells containing GFP–FTCD/vimentin fibers exhibited dramatic Golgi rearrangements (Fig. 6 C). The Golgi complex was no longer a single compact structure but appeared as an as-

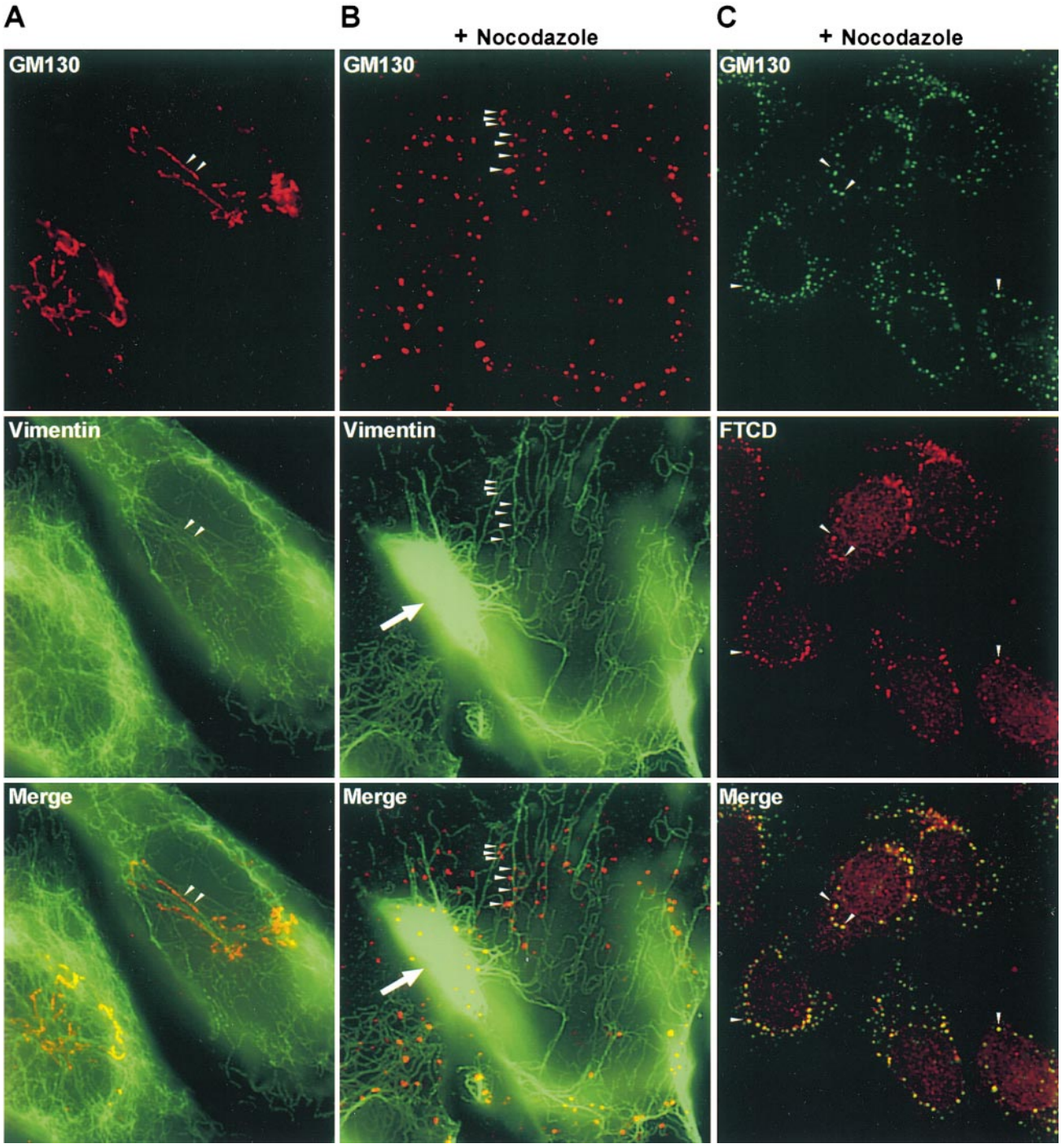

Figure 7. Golgi elements interact with vimentin filaments in vivo. (A) MFT-6 cells were labeled with polyclonal anti-GM130 and monoclonal antivimentin antibodies. Extended Golgi elements align with vimentin filaments (arrowheads). (B) MFT-6 cells were treated with 10 μg/ml nocodazole for 5 h at 37°C before labeling as in A. The Golgi complex was disrupted into Golgi ministacks, but the Golgi ministacks were associated with vimentin filaments (arrowheads). Arrow points to a mass of collapsed vimentin. (C) NRK cells were treated with 10 μg/ml nocodazole for 5 h at 37°C and then labeled with polyclonal anti-GM130 and monoclonal anti-FTCD antibodies. FTCD colocalizes with GM130 in Golgi ministacks (arrowheads).

sembly of smaller punctate or tubular elements. A proportion of the Golgi fragments were localized to the perinuclear MTOC region, but many were in more peripheral regions of cells. However, all of the Golgi elements were associated with the GFP–FTCD/vimentin filaments (arrowheads).

Our results that FTCD interacts with the Golgi complex and with vimentin IFs, and that it coordinately influences the structure of the Golgi and the vimentin IF cytoskeleton, raised the possibility that the Golgi complex and the vimentin IF cytoskeleton might interact, and that FTCD might participate in this interaction.

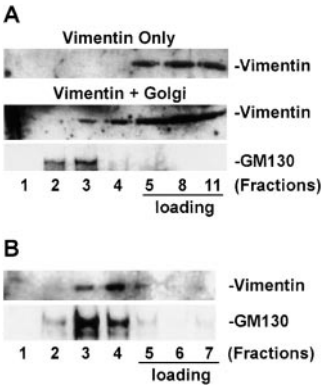

Figure 8. Golgi elements interact with vimentin filaments in vitro. (A) Recombinant vimentin alone (Vimentin only) or recombinant vimentin incubated with isolated Golgi elements (Vimentin + Golgi) were loaded at the bottom of a sucrose density gradient and subjected to equilibrium centrifugation. An equivalent amount of each fraction was processed by SDS-PAGE, transferred to NC, and immunoblotted with antivimentin and anti-GM130 antibodies. Vimentin remains in the load when centrifuged alone but is recovered in a lower density fraction containing the Golgi marker GM130 when incubated with Golgi elements. (B) Fractions 3 and 4 from A were combined, loaded at the bottom of a sucrose density gradient, and subjected to another round of equilibrium centrifugation. Fractions were collected and analysed as in A. Vimentin remains associated with Golgi elements.

Golgi Elements Associate with Vimentin IFs

To test whether Golgi elements and vimentin filaments associate in vivo, we examined mouse MFT-6 cells processed for double label immunofluorescence to detect the Golgi protein GM130 and vimentin. As shown in Fig. 7 A, MFT-6 cells have relatively large and extended Golgi complexes, with individual Golgi elements often colocalizing with vimentin IFs (arrowheads). Careful examination of distinct focal planes indicated that the majority of Golgi ribbons are closely aligned and parallel the vimentin filaments. Analogous images were observed in COS-7, NRK, and HeLa cells (data not shown), showing the generality of the Golgi–vimentin IFs association.

The observed colocalization could reflect the association of Golgi elements with microtubules, since microtubules and IFs have been previously reported to be in a parallel arrangement (Gurland and Gundersen, 1995). Therefore, to examine whether Golgi elements associate with IFs independent of microtubules, we disrupted microtubules with nocodazole and then reexamined the localization of Golgi elements and vimentin IFs. Golgi morphology and localization near the MTOC is dependent on intact microtubules (Rogalski and Singer, 1984), and disruption of microtubules results in the appearance of scattered punctate structures shown to represent Golgi ministacks (Cole et al., 1996). As shown in Fig. 7 B, in nocodazole-treated MFT-6 cells, the Golgi complex is dispersed into scattered punctate structures. Significantly, these structures are associated with vimentin filaments traversing the cells (arrowheads). Quantitation indicated that ~80% of the counted 1,032 Golgi ministacks were directly on vimentin filaments. This is likely to be an underestimate since some of the thin IFs might be out of the plane of focus and difficult to detect. Analysis of analogous sections with antitubulin antibodies indicated absence of intact microtubules (data not shown; and Fig. 4 D).

The morphologically observed association was confirmed biochemically, using a centrifugation-based Golgi–vimentin binding assay. The Golgi fraction used in this and subsequent studies is isolated from rat liver homogenate and is enriched in SG complexes as described previously (Salamero et al., 1990). Recombinant vimentin remained in high density sucrose fractions when loaded on the bottom of a discontinuous sucrose gradient and subjected to centrifugation in the absence of Golgi elements (Fig. 8 A, vimentin only, fractions 5–11). In contrast, when recombinant vimentin was incubated with isolated Golgi elements and the mixture was subjected to centrifugation, a proportion of vimentin was detected in lower density sucrose fractions (vimentin + Golgi, vimentin). These fractions contain Golgi elements as shown by enrichment in GM130 (vimentin + Golgi, GM130). To ensure that the vimentin recovered in the lower density fractions is membrane bound and does not represent contamination with soluble vimentin, fractions 3 and 4 from A were combined, loaded on the bottom of a discontinuous sucrose gradient, and subjected to another round of centrifugation. As shown in Fig. 8 B, vimentin was predominantly recovered in lower density fractions and was minimally recovered in the high density load fractions (vimentin). The lower density fractions contained Golgi elements as shown by their content of GM130 (GM130). It should be noted that within the sensitivity limits of our immunoblotting assay, the isolated Golgi fraction does not contain detectable vimentin (data not shown), suggesting that the vimentin recovered in the light density fractions bound to Golgi elements during the incubation.

Together, the morphological and biochemical results document the previously unrecognized association between Golgi elements and vimentin IFs.

FTCD Promotes Association between Golgi Elements and Vimentin IFs

The association of Golgi ministacks with vimentin filaments in vivo, and the binding of Golgi elements and vimentin in vitro, implies the presence of specific proteins that mediate the interaction. Since FTCD binds to Golgi elements and vimentin, it might serve as a linking component. In agreement, FTCD colocalizes with Golgi ministacks aligned on vimentin filaments after microtubule disruption (Fig. 7 C, arrowheads), consistent with the putative role of FTCD in tethering Golgi elements and IFs.

To explore the possible linking function of FTCD, we first tested whether FTCD can promote Golgi–vimentin interactions using a density gradient centrifugation assay. Isolated Golgi elements were supplemented either with bacterially expressed and purified FTCD or with control bacterial lysate without FTCD, loaded at the bottom of a sucrose density gradient, and centrifuged. Upfloated membranes from each group were incubated with vimentin and subjected to another round of equilibrium centrifugation. The fractions were collected and tested for their content of vimentin, GM130, and FTCD. As shown in Fig. 9 A, when Golgi elements are not preincubated with FTCD (SG + control lysate + vimentin), vimentin is predominantly recovered in the load at the bottom of the gradient (fractions 5–11), with small amount recovered in lower density fractions containing the bulk of the Golgi marker GM130 (fractions 2 and 3). A significantly different vimentin distribution pattern is obtained when Golgi elements are preincubated with FTCD. As shown in Fig. 9 A, in the presence of exogenous FTCD (SG + FTCD +

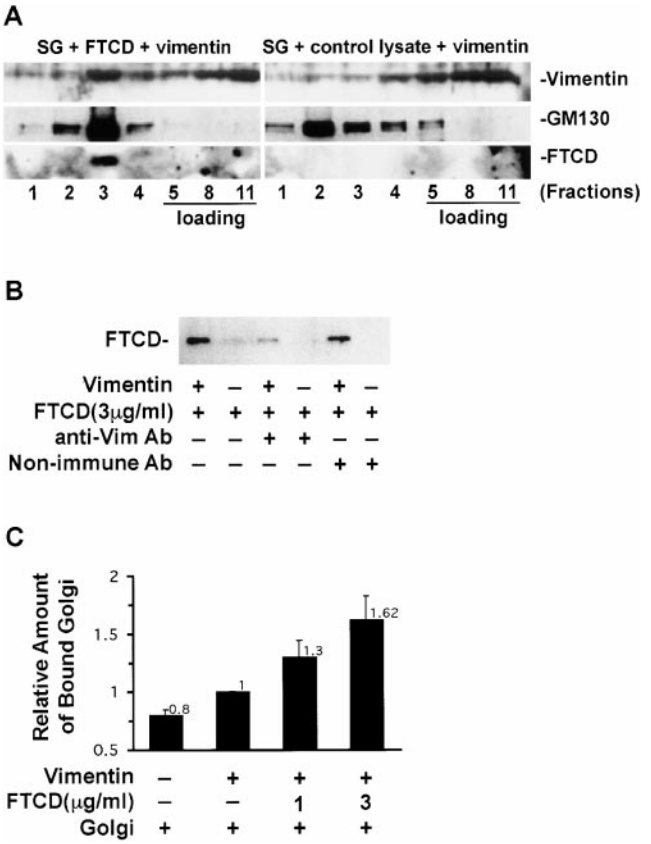

Figure 9. FTCD promotes binding of Golgi elements to vimentin. (A) Isolated Golgi elements were incubated either with bacterially expressed and purified FTCD (SG + FTCD + vimentin) or with control bacterial lysate (SG + control lysate + vimentin). The mixtures were loaded at the bottom of a sucrose density gradient and subjected to equilibrium centrifugation to separate soluble proteins from the Golgi membranes. Membrane-containing fractions were combined and supplemented with recombinant vimentin. The mixtures were loaded at the bottom of a sucrose density gradient and subjected to another equilibrium centrifugation. An equivalent amount of each fraction was processed by SDS-PAGE, transferred to NC, and immunoblotted with antivimentin, anti-GM130, and anti-FTCD antibodies. A proportion of vimentin binds to Golgi elements in the absence of exogenously added FTCD (SG + control lysate + vimentin), but vimentin binding is significantly increased by preincubating the Golgi elements with FTCD (SG + FTCD + vimentin). (B) Poly-L-lysine–coated microtiter wells containing adsorbed vimentin (+) or lacking vimentin (−) received bacterially expressed and purified FTCD, a mixture of FTCD and goat antivimentin antiserum, or a mixture of FTCD and goat nonimmune antiserum. After washing, bound material from triplicate wells was recovered with SDS-PAGE sample buffer and pooled. The pooled material was processed by SDS-PAGE, transferred to NC, and immunoblotted with anti-FTCD antibodies. Vimentin mediates FTCD binding to the wells since FTCD is recovered in wells containing adsorbed vimentin but not in wells lacking vimentin, and FTCD binding is inhibited by antivimentin antibodies. (C) Poly-L-lysine–coated microtiter wells lacking vimentin or containing adsorbed vimentin received buffer, or increasing amounts of bacterially expressed and purified FTCD. Each experimental group contained four wells. After washing to remove unbound FTCD, isolated Golgi elements were added to the wells. After washing to remove unbound Golgi elements, antigiantin antibodies and HRP-conjugated secondary antibodies were added sequentially, followed by an HRP-based colorimetric assay. Background value without Golgi addition has been subtracted from each group. The amount of Golgi binding to vimentin-containing wells without FTCD was set as 1. Each value is an average of three independent experiments, and bars indicate SD. Golgi elements preferentially bind to wells containing adsorbed vimentin, and this association is increased by FTCD in a dose-dependent manner.

vimentin), a significantly larger proportion of vimentin is recovered in the Golgi containing fractions. Vimentin is most enriched in fraction 3, which contains the bulk of Golgi elements and the bulk of bound FTCD. These data suggest that addition of FTCD promotes the association between Golgi elements and vimentin.

These results were confirmed and extended using a solid phase binding assay. To set up the assay, we tested parameters of recombinant FTCD binding to microtiter wells containing or lacking adsorbed vimentin. As shown in Fig. 9 B, significant amounts of FTCD bound to microtiter wells coated with vimentin, but minimal FTCD bound to wells without vimentin, suggesting that FTCD binds to the wells through interacting with vimentin. This was further confirmed by the finding that addition of antivimentin antibodies (to mask binding sites on vimentin) inhibited FTCD binding, whereas addition of nonimmune antibodies had no effect on FTCD binding. The results indicate that FTCD binds specifically to vimentin immobilized in microtiter wells, and that this assay can be used to test whether vimentin-bound FTCD promotes binding of Golgi elements.

First, we tested the binding of Golgi elements to microtiter wells in the absence of vimentin or FTCD. Basal level of binding was observed (Fig. 9 C), and this represents the background in this analysis. Increased binding of Golgi elements was observed when microtiter wells containing adsorbed vimentin were tested, most likely reflecting binding through intrinsic elements on the Golgi membrane. This finding is in agreement with data presented in Fig. 8 A, showing that vimentin and Golgi elements interact in a centrifugation-based assay. Significantly, adding recombinant FTCD to the vimentin-containing wells before adding Golgi elements led to a dose-dependent (>130% at 1 μg/ml FTCD and >160% at 3.5 μg/ml FTCD) increase in Golgi elements binding. Together, the data indicate that FTCD promotes binding between Golgi elements and vimentin.

Discussion

Structural and functional interactions between the Golgi complex and the microtubule and the actin cytoskeletal systems have been documented. The structure of the Golgi complex and its localization adjacent to the MTOC is dependent on intact microtubules since disruption of the microtubule cytoskeleton leads to fragmentation of the single Golgi complex into numerous Golgi ministacks scattered throughout the cell (reviewed in Kreis, 1990; Cole et al., 1996). Although the interaction of Golgi elements with the actin cytoskeleton is less understood, components of the actin-associated cytoskeleton such as a β-spectrin isoform (Beck et al., 1994) and ankyrin isoforms (Devarajan et al., 1996; Holleran et al., 1996) have

been shown to preferentially localize to the Golgi complex, suggesting a link.

Interactions between the Golgi complex and the IF cytoskeleton have not been extensively studied. Here, we document the novel association of Golgi elements with vimentin filaments and show that the peripherally associated Golgi protein FTCD directly interacts with vimentin filaments and can coordinately remodel the vimentin IF cytoskeleton and the Golgi complex. Our results suggest that Golgi elements interface with the IF cytoskeleton and that FTCD participates in coupling Golgi membranes to vimentin filaments.

Golgi Ribbons and Golgi Ministacks Associate with Vimentin Filaments

It has been shown by stereo EM and computer graphic reconstruction that vimentin filaments and microtubules are abundant in close vicinity to the Golgi complex, and some appear intimately associated with the Golgi membrane (Katsumoto et al., 1991). The close alignment between IFs and the Golgi complex was also seen by scanning EM (Takumida and Anniko, 1994; Takumida and Anniko, 1996). However, since IFs and microtubules often parallel each other (Blose et al., 1984; Gurland and Gundersen, 1995), the alignment between Golgi elements and IFs could reflect Golgi association with microtubules rather than IFs. We explored whether Golgi complexes directly interact with IFs by examining Golgi localization in cells lacking an intact microtubule cytoskeleton and containing numerous Golgi ministacks scattered throughout the cell (Cole et al., 1996). Significantly, the Golgi ministacks were associated with vimentin filaments, suggesting that Golgi elements interact with vimentin filaments independently of the microtubule cytoskeleton.

What might be the significance of linking Golgi elements to the vimentin cytoskeleton? It is clear that Golgi structure and function are not fundamentally dependent on the vimentin IFs since, in $vim^{-/-}$ MFT-16 cells, the Golgi complexes appear normal (data not shown), and the vimentin knockout mouse appears to maintain normal secretory functions (Colucci-Guyon et al., 1994). However, as shown here, rearrangement of the vimentin IF cytoskeleton is paralleled by changes in Golgi structure, suggesting that the Golgi complex and the IF cytoskeleton are linked and that a hierarchy of interactions involving all three cytoskeletal systems might modulate Golgi structure and function in vivo. The microtubule cytoskeleton appears most important since perturbations cause complete disruption of Golgi structure and significant decrease in secretory function (Rogalski and Singer, 1984). More subtle defects are seen when Golgi interactions with the actin cytoskeleton are perturbed: in cells in which dominant negative mutants of Golgi-specific spectrin isoforms are expressed, the Golgi structure remains relatively normal, but the trafficking of the α and the β subunits of Na, K-ATPase, and the VSV-G protein through the Golgi seems impaired (Devarajan et al., 1997). It is likely that linking Golgi elements to vimentin IFs is also required for the more subtle functions of the organelle. For example, studies examining glycolipid synthesis have documented that, in $vim^{-/-}$ cells, the intracellular transport of glycolipids between the endosomal/lysosomal pathway and the Golgi complex appears impaired (Gillard et al., 1998). Thus, interactions between the Golgi and the IFs might integrate the secretory pathway with the IF cytoskeleton, consequently coordinating the efficiency and fidelity of membrane traffic with the motility, adhesion, and/or polarity status of the cell.

FTCD Represents a Novel Type of Golgi Complex–associated IFAP

We consider the peripherally associated Golgi protein FTCD an IFAP since it binds directly to vimentin subunits and to polymerized vimentin, integrates into vimentin-based filaments, and dramatically changes the structure of the vimentin IF cytoskeleton.

The most extensively studied IFAPs are those belonging to a related family of plakins characterized by a conserved overall structure and partial sequence homology. Plectin mediates the interaction of vimentin IFs with actin- and microtubule-based filaments, as well as with specialized membrane adhesion zones (Foisner et al., 1995; Svitkina et al., 1996). A related protein, filamin, links vimentin IFs only to actin filaments (Brown and Binder, 1992), whereas the desmosomal plague component, desmoplakin, might link vimentin IFs to the adhesion zone (Stappenbeck and Green, 1992; Stappenbeck et al., 1993). In addition to plakins, other proteins also interact with vimentin. Specific kinases, including PKC β (Murti et al., 1992; Spudich et al., 1992) and PKC ϵ isoforms (Owen et al., 1996), cGMP kinase (Pryzwansky et al., 1995), and Yes kinase (Ciesielski-Treska et al., 1995), a nucleoside diphosphate kinase (Otero, 1997), a transglutaminase (Trejo-Skalli et al., 1995; Clement et al., 1998), proteins related to the small heat shock protein family, α-crystallins (Nicholl and Quinlan, 1994; Perng et al., 1999), and the actin-binding protein fimbrin (Correia et al., 1999), bind to vimentin and might participate in modulating the organization or the dynamics of IF assembly. Based on the structural heterogeneity of various vimentin-binding proteins, it is likely that a spatially relevant conformation might mediate vimentin binding or that many distinct binding motifs can be used. The molecular basis of FTCD interaction with vimentin is not obvious, based on its primary structure, since FTCD has no sequence homology with any previously characterized IFAP.

FTCD participation in vimentin-based events was unexpected since FTCD has been studied predominantly as a bifunctional enzyme involved in the degradation of histidine (MacKenzie et al., 1980). The two enzymatic activities of FTCD reside in a single polypeptide chain, with the transferase domain at the NH_2-terminal region, connected by a short region to the deaminase domain at the COOH terminus (Murley and MacKenzie, 1995). Dimerization is required for each monofunctional activity, but the overall enzymatic property of FTCD is further regulated by its assembly into a planar octamer (Beaudet and MacKenzie, 1976; MacKenzie et al., 1980; Findlay and MacKenzie, 1987, 1988). Although the involvement of a FTCD in regulating vimentin filament dynamics was unexpected, it has a precedent: mutations in the enzyme superoxide dismutase have been shown to cause accumulation of neurofilaments in neurons and result in amyotrophic lateral sclerosis (for review see Cleveland, 1999). This effect was not dependent on the enzymatic activity of the protein, suggesting that superoxide dismutase performs other cellular functions relevant for neurofilament dynamics. Similarly, FTCD might

perform multiple cellular functions, including participation in the organization and/or assembly of the vimentin IF cytoskeleton.

FTCD Influences the Structure of the Vimentin IF Cytoskeleton

Normally, the vimentin IF cytoskeleton consists of anastomosing arrays of fibers, usually concentrated around the nucleus and the peri-Golgi region and extending in irregular networks towards the cell periphery. In FTCD expressing cells, thick FTCD/vimentin fibers originate from the peri-Golgi region and either extend towards the periphery or coil around the nucleus and cell core. Formation of the fibers is concurrent with significant depletion of peripheral vimentin elements. The changes in the IF cytoskeleton are not secondary effects caused by alterations in the actin or microtubule cytoskeletons, since these networks appear unperturbed by FTCD expression. The lack of microtubule disruption was especially relevant since the FTCD effect superficially resembled the pattern seen in cells in which the microtubule cytoskeleton was collapsed by depolymerization of microtubules (Gurland and Gundersen, 1995) or interference with kinesin, a microtubule-based motor protein shown to mediate peripheral extension of vimentin IFs on microtubules (Gyoeva and Gelfand, 1991; Liao and Gundersen, 1998). These results imply that, in FTCD-transfected cells, the interactions of IFAPs that normally cross-link IFs to actin or microtubule systems is severed. Whether this is accomplished by FTCD displacing the IFAPs from the vimentin binding sites, or by other events, remains to be investigated and will provide mechanistic insight into how different IFAPs, including FTCD, control vimentin IF dynamics. The aberrant FTCD/vimentin fibers are also not novel forms of aggresome, a structure that appears to recruit vimentin filaments to its surface (data not show; Garcia-Mata et al., 1999; Johnston et al., 1998).

The formation of thick FTCD/vimentin fibers in vivo and the ability of recombinant FTCD to bridge vimentin filaments in vitro suggest that FTCD mediates cross-linking of vimentin filaments into higher order structures. In agreement, we observed that expression of FTCD causes bundling of individual FTCD/vimentin fibers when imaged in real time in vivo (data not shown). The cross-linking function of FTCD is consistent with its oligomeric structure, planar shape, and size. The FTCD bagel-like ring of eight identical subunits is arranged as a tetramer of dimers. If each FTCD dimer interacts with a different vimentin filament simultaneously, the octamer could cross-link four vimentin filaments. Negative staining EM of native FTCD shows an ~12-nm-diam ring (Beaudet and MacKenzie, 1976; MacKenzie et al., 1980), and these dimensions are theoretically large enough to cross-link four individual 10-nm vimentin filaments.

FTCD Integrates Golgi Elements with Vimentin IFs

FTCD fulfills five major criteria expected of a protein participating in linking Golgi membranes and vimentin filaments.

(1) FTCD localizes to relevant cellular compartments. Endogenous FTCD is concentrated in the Golgi region by immunofluorescence (Bloom and Brashear, 1989; Gao et al., 1998; Hennig et al., 1998). However, reexamination of FTCD distribution showed that endogenous and recombinant FTCD localize to the Golgi stack and also to vimentin filaments distributed throughout the cells. Interestingly, in BFA-treated cells in which the Golgi complex is partially disrupted, FTCD associates with filamentous structures originating from the peri-Golgi region (Gao et al., 1998). This result supports the idea that FTCD localizes to Golgi membranes but redistributes to filaments when the Golgi complex is disrupted. Similar behavior has been observed for plectin, which can interact with IFs and with microtubules; in normal cells, plectin preferentially colocalizes with IFs, but, in cells which do not contain vimentin, plectin binds to microtubules (Svitkina et al., 1996).

(2) FTCD associates with Golgi membranes. A proportion of cellular FTCD is recovered with Golgi membranes during fractionation, whereas the majority of FTCD is recovered in the supernatant cytosolic fraction (Bloom and Brashear, 1989; Gao et al., 1998; Hennig et al., 1998). It is most likely that FTCD binds to Golgi membranes through protein–protein interactions, since FTCD does not contain motifs capable of mediating direct lipid interactions. The identity of the Golgi membrane receptor for FTCD is currently unknown, but the protein(s) mediating FTCD binding are not regulated by guanine exchange factors (for review see Jackson and Casanova, 2000), since treatment of cells with the drug BFA known to inhibit the activity of such factors (Donaldson et al., 1992; Franco et al., 1998) does not cause FTCD to dissociate from the membranes (Gao et al., 1998).

(3) FTCD interacts with vimentin. We document the novel finding that FTCD binds directly to vimentin subunits and to vimentin filaments, integrates into chimeric FTCD/vimentin fibers, and markedly disrupts the vimentin IF cytoskeleton. The interacting regions of FTCD and vimentin have not been yet defined. Preliminary results (data not shown) suggest that the native FTCD octamer might be required for fiber formation since expression of FT or CD domains alone does not lead to FTCD/vimentin fiber formation.

(4) FTCD coordinately modulates the structure of the Golgi complex and the vimentin IF cytoskeleton. A prediction of a linking function for FTCD would be that FTCD present in FTCD/vimentin fibers could interact with Golgi elements and cause changes in Golgi morphology. Indeed, in cells containing FTCD/vimentin fibers, Golgi structure was disrupted to a varying degree with Golgi membranes aligned along the FTCD/vimentin fibers. It should be stressed that the formation of the FTCD/vimentin fibers did not cause microtubule rearrangements and, therefore, the disruption in Golgi structure was a direct result of alterations in the vimentin IF cytoskeleton. The coordinate change in organellar morphology as a result of cytoskeletal perturbation is not unique to the Golgi complex and the IF cytoskeleton, and previous studies have documented that overexpression of proteins linking membranous organelles to the microtubule cytoskeleton or the actin cytoskeletons cause changes in the cytoskeleton and the organelle. For example, coordinate perturbations in Golgi structure and microtubule bundling were observed in cells overexpressing the peripheral Golgi protein GMAP-210 (Infante et al., 1999). Similarly, in cells

overexpressing the ER membrane protein CLIMP-63, bundling of microtubules was paralleled by the rearrangement of ER elements along the microtubule bundles (Klopfenstein et al., 1998). Similarly, overexpression of the actin-related protein centractin caused the formation of abnormal centractin filaments and resulted in Golgi disruption and coalignment of Golgi elements on the centractin filaments (Holleran et al., 1996).

(5) FTCD promotes interaction between Golgi elements and vimentin. We show that addition of FTCD preferentially increases binding of Golgi elements and vimentin in a centrifugation and solid state binding assays. Since FTCD binds to Golgi elements and to vimentin, the simplest interpretation of this result is that FTCD acts as a molecular bridge linking Golgi membranes and vimentin. However, we can not exclude the possibility that FTCD might modify the Golgi surface in a way that allows direct binding of Golgi elements to vimentin. In both cases, FTCD facilitates the Golgi–vimentin interaction, and thus fundamentally participates in the tethering event.

Our results support a model in which FTCD acts as a structural–functional interface between Golgi elements and the IF cytoskeleton. FTCD may modulate the extension of Golgi cisternae along IF filaments or may stabilize the extended cisternae by directly anchoring them to IFs. FTCD might also regulate the ability of Golgi elements to interact with the various cytoskeletal systems by preventing or allowing the dynamic interactions of Golgi membranes with the microtubule-based cytoskeletal system, the spectrin/actin–based cytoskeletal system, or with other Golgi-specific cytoskeletal proteins exemplified by p230 (Erlich et al., 1996), golgin-97 (Griffith et al., 1997), giantin (Linstedt and Hauri, 1993), and GM130 (Nakamura et al., 1995). Further analysis will be required to explore the exact molecular mechanism of FTCD action.

We thank Dr. Robert Evans for critically evaluating the manuscript, and Dr. James Collawn for helpful comments on the manuscript.

Submitted: 26 June 2000
Revised: 4 December 2000
Accepted: 5 January 2001

References

Alvarez, C., H. Fujita, A. Hubbard, and E. Sztul. 1999. ER to Golgi transport: requirement for p115 at a pre-Golgi VTC stage. *J. Cell Biol.* 147:1205–1222.

Bashour, A.M., and G.S. Bloom. 1998. 58K, a microtubule-binding Golgi protein, is a formiminotransferase cyclodeaminase. *J. Biol. Chem.* 273:19612–19617.

Beaudet, R., and R.E. Mackenzie. 1976. Formiminotransferase cyclodeaminase from porcine liver. An octomeric enzyme containing bifunctional polypeptides. *Biochim. Biophys. Acta.* 453:151–161.

Beck, K.A., J.A. Buchanan, V. Malhotra, and W.J. Nelson. 1994. Golgi spectrin: identification of an erythroid beta-spectrin homologue associated with the Golgi complex. *J. Cell Biol.* 127:707–723.

Bloom, G.S., and T.A. Brashear. 1989. A novel 58-kDa protein associates with the Golgi apparatus and microtubules. *J. Biol. Chem.* 264:16083–16092.

Blose, S.H., D.I. Meltzer, and J.R. Feramisco. 1984. 10-nm filaments are induced to collapse in living cells microinjected with monoclonal and polyclonal antibodies against tubulin. *J. Cell Biol.* 98:847–858.

Brown, K.D., and L.I. Binder. 1992. Identification of the intermediate filament-associated protein gyronemin as filamin. Implications for a novel mechanism of cytoskeletal interaction. *J. Cell Sci.* 102:19–30.

Chou, Y.H., O. Skalli, and R.D. Goldman. 1997. Intermediate filaments and cytoplasmic networking: new connections and more functions. *Curr. Opin. Cell Biol.* 9:49–53.

Ciesielski-Treska, J., G. Ulrich, S. Chasserot-Golaz, and D. Aunis. 1995. Immunocytochemical localization of protein kinases Yes and Src in amoeboid microglia in culture: association of Yes kinase with vimentin intermediate filaments. *Eur. J. Cell Biol.* 68:369–376.

Clement, S., P.T. Velasco, S.N. Murthy, J.H. Wilson, T.J. Lukas, R.D. Goldman, and L. Lorand. 1998. The intermediate filament protein, vimentin, in the lens is a target for cross-linking by transglutaminase. *J. Biol. Chem.* 273: 7604–7609.

Cleveland, D.W. 1999. From Charcot to SOD1: mechanisms of selective motor neuron death in ALS. *Neuron.* 24:515–520.

Cole, N.B., N. Sciaky, A. Marotta, J. Song, and J. Lippincott-Schwartz. 1996. Golgi dispersal during microtubule disruption: regeneration of Golgi stacks at peripheral endoplasmic reticulum exit sites. *Mol. Biol. Cell.* 7:631–650.

Colucci-Guyon, E., M.M. Portier, I. Dunia, D. Paulin, S. Pournin, and C. Babinet. 1994. Mice lacking vimentin develop and reproduce without an obvious phenotype. *Cell.* 79:679–694.

Correia, I., D. Chu, Y.H. Chou, R.D. Goldman, and P. Matsudaira. 1999. Integrating the actin and vimentin cytoskeletons: adhesion-dependent formation of fimbrin–vimentin complexes in macrophages. *J. Cell Biol.* 146:831–842.

Devarajan, P., P.R. Stabach, A.S. Mann, T. Ardito, M. Kashgarian, and J.S. Morrow. 1996. Identification of a small cytoplasmic ankyrin (AnkG119) in the kidney and muscle that binds beta I sigma spectrin and associates with the Golgi apparatus. *J. Cell Biol.* 133:819–830.

Devarajan, P., P.R. Stabach, M.A. De Matteis, and J.S. Morrow. 1997. Na,K-ATPase transport from endoplasmic reticulum to Golgi requires the Golgi spectrin-ankyrin G119 skeleton in Madin Darby canine kidney cells. *Proc. Natl. Acad. Sci. USA.* 94:10711–10716.

Domingo A., A.J. Sarria., R.M. Evans, and M.W. Klymkowsky. 1991. Studying intermediate filaments. *In* The Cytoskeleton: A Practical Approach. K. Carraway and C. Carraway, editors. Oxford University Press, Washington D.C. 223–255.

Donaldson, J.G., J. Lippincott-Schwartz, G.S. Bloom, T.E. Kreis, and R.D. Klausner. 1990. Dissociation of a 110-kD peripheral membrane protein from the Golgi apparatus is an early event in brefeldin A action. *J. Cell Biol.* 111: 2295–2306.

Donaldson, J.G., D. Finazzi, and R.D. Klausner. 1992. Brefeldin A inhibits Golgi membrane-catalysed exchange of guanine nucleotide onto ARF protein. *Nature.* 360:350–352.

Erlich, R., P.A. Gleeson, P. Campbell, E. Dietzsch, and B.H. Toh. 1996. Molecular characterization of trans-Golgi p230. A human peripheral membrane protein encoded by a gene on chromosome 6p12-22 contains extensive coiled-coil alpha-helical domains and a granin motif. *J. Biol. Chem.* 271: 8328–8337.

Findlay, W.A., and R.E. MacKenzie. 1987. Dissociation of the octameric bifunctional enzyme formiminotransferase-cyclodeaminase in urea. Isolation of two monofunctional dimers. *Biochemistry.* 26:1948–1954.

Findlay, W.A., and R.E. MacKenzie. 1988. Renaturation of formiminotransferase-cyclodeaminase from guanidine hydrochloride. Quaternary structure requirements for the activities and polyglutamate specificity. *Biochemistry.* 27:3404–3408.

Foisner, R., W. Bohn, K. Mannweiler, and G. Wiche. 1995. Distribution and ultrastructure of plectin arrays in subclones of rat glioma C6 cells differing in intermediate filament protein (vimentin) expression. *J. Struct. Biol.* 115:304–317.

Franco, M., J. Boretto, S. Robineau, S. Monier, B. Goud, P. Chardin, and P. Chavrier. 1998. ARNO3, a Sec7-domain guanine nucleotide exchange factor for ADP ribosylation factor 1, is involved in the control of Golgi structure and function. *Proc. Natl. Acad. Sci. USA.* 95:9926–9931.

Franke, W.W., E. Schmid, S. Winter, M. Osborn, and K. Weber. 1979. Widespread occurrence of intermediate-sized filaments of the vimentin type in cultured cells from diverse vertebrates. *Exp. Cell Res.* 123:25–46.

Franke, W.W., C. Grund, C. Kuhn, B.W. Jackson, and K. Illmensee. 1982. Formation of cytoskeletal elements during mouse embryogenesis. III. Primary mesenchymal cells and the first appearance of vimentin filaments. *Differentiation.* 23:43–59.

Fuchs, E., and K. Weber. 1994. Intermediate filaments: structure, dynamics, function, and disease. *Annu. Rev. Biochem.* 63:345–382.

Galou, M., E. Colucci-Guyon, D. Ensergueix, J.L. Ridet, M. Gimenez y Ribotta, A. Privat, C. Babinet, and P. Dupouey. 1996. Disrupted glial fibrillary acidic protein network in astrocytes from vimentin knockout mice. *J. Cell Biol.* 133:853–863.

Gao, Y.S., C. Alvarez, D.S. Nelson, and E. Sztul. 1998. Molecular cloning, characterization, and dynamics of rat formiminotransferase cyclodeaminase, a Golgi-associated 58-kDa protein. *J. Biol. Chem.* 273:33825–33834.

Garcia-Mata, R., Z. Bebok, E.J. Sorscher, and E.S. Sztul. 1999. Characterization and dynamics of aggresome formation by a cytosolic GFP–chimera. *J. Cell Biol.* 146:1239–1254.

Georgatos, S.D., and C. Maison. 1996. Integration of intermediate filaments into cellular organelles. *Int. Rev. Cytol.* 164:91–138.

Gillard, B.K., R. Clement, E. Colucci-Guyon, C. Babinet, G. Schwarzmann, T. Taki, T. Kasama, and D.M. Marcus. 1998. Decreased synthesis of glycosphingolipids in cells lacking vimentin intermediate filaments. *Exp. Cell Res.* 242:561–572.

Gomi, H., T. Yokoyama, K. Fujimoto, T. Ikeda, A. Katoh, T. Itoh, and S. Itohara. 1995. Mice devoid of the glial fibrillary acidic protein develop normally and are susceptible to scrapie prions. *Neuron.* 14:29–41.

Griffith, K.J., E.K. Chan, C.C. Lung, J.C. Hamel, X. Guo, K. Miyachi, and M.J. Fritzler. 1997. Molecular cloning of a novel 97-kd Golgi complex autoanti-

gen associated with Sjogren's syndrome. *Arthritis Rheum*. 40:1693–1702.
Gurland, G., and G.G. Gundersen. 1995. Stable, detyrosinated microtubules function to localize vimentin intermediate filaments in fibroblasts. *J. Cell Biol*. 131:1275–1290.
Gyoeva, F.K., and V.I. Gelfand. 1991. Coalignment of vimentin intermediate filaments with microtubules depends on kinesin. *Nature*. 353:445–448.
Hennig, D., S.J. Scales, A. Moreau, L.L. Murley, J. De Mey, and T.E. Kreis. 1998. A formiminotransferase cyclodeaminase isoform is localized to the Golgi complex and can mediate interaction of trans-Golgi network-derived vesicles with microtubules. *J. Biol. Chem*. 273:19602–19611.
Holleran, E.A., M.K. Tokito, S. Karki, and E.L. Holzbaur. 1996. Centractin (ARP1) associates with spectrin revealing a potential mechanism to link dynactin to intracellular organelles. *J. Cell Biol*. 135:1815–1829.
Holwell, T.A., Schweitzer, S.C., and R.M. Evans. 1997. Tetracycline regulated expression of vimentin in fibroblasts derived from vimentin null mice. *J. Cell Sci.* 110:1947–1956.
Infante, C., F. Ramos-Morales, C. Fedriani, M. Bornens, and R.M. Rios. 1999. GMAP-210, A cis-Golgi network–associated protein, is a minus end microtubule-binding protein. *J. Cell Biol*. 145:83–98.
Jackson, C.L., and J.E. Casanova. 2000. Turning on ARF: the Sec7 family of guanine-nucleotide-exchange factors. *Trends Cell Biol*. 10:60–67.
Johnston, J.A., C.L. Ward, and R.R. Kopito. 1998. Aggresomes: a cellular response to misfolded proteins. *J. Cell Biol*. 143:1883–1898.
Katsumoto, T., M. Inoue, T. Naguro, and T. Kurimura. 1991. Association of cytoskeletons with the Golgi apparatus: three-dimensional observation and computer-graphic reconstruction. *J. Electron Microsc.* 40:24–28.
Klopfenstein, D.R., F. Kappeler, and H.P. Hauri. 1998. A novel direct interaction of endoplasmic reticulum with microtubules. *EMBO (Eur. Mol. Biol. Organ.) J*. 17:6168–6177.
Kreis, T.E. 1990. Role of microtubules in the organisation of the Golgi apparatus. *Cell Motil. Cytoskeleton*. 15:67–70.
Kreitzer, G., G. Liao, and G.G. Gundersen. 1999. Detyrosination of tubulin regulates the interaction of intermediate filaments with microtubules in vivo via a kinesin-dependent mechanism. *Mol. Biol. Cell*. 10:1105–1118.
Leung, C.L., D. Sun, and R.K. Liem. 1999. The intermediate filament protein peripherin is the specific interaction partner of mouse BPAG1-n (dystonin) in neurons. *J. Cell Biol*. 144:435–446.
Li, H., S.K. Choudhary, D.J. Milner, M.I. Munir, I.R. Kuisk, and Y. Capetanaki. 1994. Inhibition of desmin expression blocks myoblast fusion and interferes with the myogenic regulators MyoD and myogenin. *J. Cell Biol*. 124: 827–841.
Liao, G., and G.G. Gundersen. 1998. Kinesin is a candidate for cross-bridging microtubules and intermediate filaments. Selective binding of kinesin to detyrosinated tubulin and vimentin. *J. Biol. Chem*. 273:9797–9803.
Lieber, J.G., and R.M. Evans. 1996. Disruption of the vimentin intermediate filament system during adipose conversion of 3T3-L1 cells inhibits lipid droplet accumulation. *J. Cell Sci*. 109:3047–3058.
Liedtke, W., W. Edelmann, P.L. Bieri, F.C. Chiu, N.J. Cowan, R. Kucherlapati, and C.S. Raine. 1996. GFAP is necessary for the integrity of CNS white matter architecture and long-term maintenance of myelination. *Neuron*. 17:607–615.
Linstedt, A.D., and H.P. Hauri. 1993. Giantin, a novel conserved Golgi membrane protein containing a cytoplasmic domain of at least 350 kDa. *Mol. Biol. Cell*. 4:679–693.
Lippincott-Schwartz, J., J.G. Donaldson, A. Schweizer, E.G. Berger, H.P. Hauri, L.C. Yuan, and R.D. Klausner. 1990. Microtubule-dependent retrograde transport of proteins into the ER in the presence of brefeldin A suggests an ER recycling pathway. *Cell*. 60:821–836.
MacKenzie, R.E., M. Aldridge, and J. Paquin. 1980. The bifunctional enzyme formiminotransferase-cyclodeaminase is a tetramer of dimers. *J. Biol. Chem*. 255:9474–9478.
Milner, D.J., G. Weitzer, D. Tran, A. Bradley, and Y. Capetanaki. 1996. Disruption of muscle architecture and myocardial degeneration in mice lacking desmin. *J. Cell Biol*. 134:1255–1270.
Murley, L.L., and R.E. MacKenzie. 1995. The two monofunctional domains of octameric formiminotransferase-cyclodeaminase exist as dimers. *Biochemistry*. 34:10358–10364.
Murley, L.L., N.R. Mejia, and R.E. MacKenzie. 1993. The nucleotide sequence of porcine formiminotransferase cyclodeaminase. Expression and purification from Escherichia coli. *J. Biol. Chem*. 268:22820–22824.
Murti, K.G., K. Kaur, and R.M. Goorha. 1992. Protein kinase C associates with intermediate filaments and stress fibers. *Exp. Cell Res*. 202:36–44.
Nakamura, N., C. Rabouille, R. Watson, T. Nilsson, N. Hui, P. Slusarewicz, T.E. Kreis, and G. Warren. 1995. Characterization of a cis-Golgi matrix protein, GM130. *J. Cell Biol*. 131:1715–1726.
Nelson, D.S., C. Alvarez, Y.S. Gao, R. Garcia-Mata, E. Fialkowski, and E. Sztul. 1998. The membrane transport factor TAP/p115 cycles between the Golgi and earlier secretory compartments and contains distinct domains required for its localization and function. *J. Cell Biol*. 143:319–331.
Nicholl, I.D., and R.A. Quinlan. 1994. Chaperone activity of alpha-crystallins modulates intermediate filament assembly. *EMBO (Eur. Mol. Biol. Organ.) J*. 13:945–953.
Nikolic, B., E. Mac Nulty, B. Mir, and G. Wiche. 1996. Basic amino acid residue cluster within nuclear targeting sequence motif is essential for cytoplasmic plectin–vimentin network junctions. *J. Cell Biol*. 134:1455–1467.
Otero, A.S. 1997. Copurification of vimentin, energy metabolism enzymes, and a MER5 homolog with nucleoside diphosphate kinase. Identification of tissue-specific interactions. *J. Biol. Chem*. 272:14690–14694.
Owen, P.J., G.D. Johnson, and J.M. Lord. 1996. Protein kinase C-delta associates with vimentin intermediate filaments in differentiated HL60 cells. *Exp. Cell Res*. 225:366–373.
Pekny, M., P. Leveen, M. Pekna, C. Eliasson, C.H. Berthold, B. Westermark, and C. Betsholtz. 1995. Mice lacking glial fibrillary acidic protein display astrocytes devoid of intermediate filaments but develop and reproduce normally. *EMBO (Eur. Mol. Biol. Organ.) J*. 14:1590–1598.
Pekny, M., C.B. Johansson, C. Eliasson, J. Stakeberg, A. Wallen, T. Perlmann, U. Lendahl, C. Betsholtz, C.H. Berthold, and J. Frisen. 1999. Abnormal reaction to central nervous system injury in mice lacking glial fibrillary acidic protein and vimentin. *J. Cell Biol*. 145:503–514.
Perng, M.D., L. Cairns, I.P. van den, A. Prescott, A.M. Hutcheson, and R.A. Quinlan. 1999. Intermediate filament interactions can be altered by HSP27 and alphaB-crystallin. *J. Cell Sci*. 112:2099–2112.
Plutner, H., H.W. Davidson, J. Saraste, and W.E. Balch. 1992. Morphological analysis of protein transport from the ER to Golgi membranes in digitonin-permeabilized cells: role of the P58 containing compartment. *J. Cell Biol*. 119:1097–1116.
Prahlad, V., M. Yoon, R.D. Moir, R.D. Vale, and R.D. Goldman. 1998. Rapid movements of vimentin on microtubule tracks: kinesin-dependent assembly of intermediate filament networks. *J. Cell Biol*. 143:159–170.
Pryzwansky, K.B., T.A. Wyatt, and T.M. Lincoln. 1995. Cyclic guanosine monophosphate-dependent protein kinase is targeted to intermediate filaments and phosphorylates vimentin in A23187-stimulated human neutrophils. *Blood*. 85:222–230.
Rogalski, A.A., and S.J. Singer. 1984. Associations of elements of the Golgi apparatus with microtubules. *J. Cell Biol*. 99:1092–1100.
Salamero, J., E.S. Sztul, and K.E. Howell. 1990. Exocytic transport vesicles generated in vitro from the trans-Golgi network carry secretory and plasma membrane proteins. *Proc. Natl. Acad. Sci. USA*. 87:7717–7721.
Sarria, A.J., S.R. Panini, and R.M. Evans. 1992. A functional role for vimentin intermediate filaments in the metabolism of lipoprotein-derived cholesterol in human SW-13 cells. *J. Biol. Chem*. 267:19455–19463.
Shane, B., and E.L.R. Stokstad. 1984. Folates in the synthesis and catabolism of histidine. *In* Folates and Pterins. Vol. 1. R.L. Blakey and S.J. Benkovic, editors. John Wiley & Sons, New York. 433–455.
Shibuki, K., H. Gomi, L. Chen, S. Bao, J.J. Kim, H. Wakatsuki, T. Fujisaki, K. Fujimoto, A. Katoh, T. Ikeda, C. Chen, R.F. Thompson, and S. Itohara. 1996. Deficient cerebellar long-term depression, impaired eyeblink conditioning, and normal motor coordination in GFAP mutant mice. *Neuron*. 16: 587–599.
Solans, A., X. Estivill, and S. de La Luna. 2000. Cloning and characterization of human FTCD on 21q22.3, a candidate gene for glutamate formiminotransferase deficiency. *Cytogenet. Cell Genet*. 88:43–49.
Spudich, A., T. Meyer, and L. Stryer. 1992. Association of the beta isoform of protein kinase C with vimentin filaments. *Cell Motil. Cytoskeleton*. 22:250–256.
Stappenbeck, T.S., and K.J. Green. 1992. The desmoplakin carboxyl terminus coaligns with and specifically disrupts intermediate filament networks when expressed in cultured cells. *J. Cell Biol*. 116:1197–1209.
Stappenbeck, T.S., E.A. Bornslaeger, C.M. Corcoran, H.H. Luu, M.L. Virata, and K.J. Green. 1993. Functional analysis of desmoplakin domains: specification of the interaction with keratin versus vimentin intermediate filament networks. *J. Cell Biol*. 123:691–705.
Svitkina, T.M., A.B. Verkhovsky, and G.G. Borisy. 1996. Plectin sidearms mediate interaction of intermediate filaments with microtubules and other components of the cytoskeleton. *J. Cell Biol*. 135:991–1007.
Sztul, E.S., K.E. Howell, and G.E. Palade. 1985. Biogenesis of the polymeric IgA receptor in rat hepatocytes. I. Kinetic studies of its intracellular forms. *J. Cell Biol*. 100:1248–1254.
Takumida, M., and M. Anniko. 1994. Cytoskeletal organization of the vestibular supporting cells. Saponin perfusion method for observing intracellular structures by scanning electron microscopy. *Acta Otolaryngol*. 114:150–155.
Takumida, M., and M. Anniko. 1996. The effect of gentamicin on cytoskeletons in the vestibular sensory cells: a high-resolution scanning electron microscopic investigation. *Acta Otolaryngol*. 116:817–823.
Trejo-Skalli, A.V., P.T. Velasco, S.N. Murthy, L. Lorand, and R.D. Goldman. 1995. Association of a transglutaminase-related antigen with intermediate filaments. *Proc. Natl. Acad. Sci. USA*. 92:8940–8944.
Vaisberg, E.A., P.M. Grissom, and J.R. McIntosh. 1996. Mammalian cells express three distinct dynein heavy chains that are localized to different cytoplasmic organelles. *J. Cell Biol*. 133:831–842.
Yang, Y., J. Dowling, Q.C. Yu, P. Kouklis, D.W. Cleveland, and E. Fuchs. 1996. An essential cytoskeletal linker protein connecting actin microfilaments to intermediate filaments. *Cell*. 86:655–665.
Yang, Y., C. Bauer, G. Strasser, R. Wollman, J.P. Julien, and E. Fuchs. 1999. Integrators of the cytoskeleton that stabilize microtubules. *Cell*. 98:229–238.